UNIVERSIDAD DE CHILE
FACULTAD DE CIENCIAS FÍSICAS Y MATEMÁTICAS
DEPARTAMENTO DE GEOLOGÍA

OPTIMIZACION DE TECNOLOGÍA DAS EN LABORATORIO PARA RETENCIÓN DE SULFATO Y METALES DE DRENAJE ACIDO DE MINAS ANDINOS UTILIZANDO RESIDUOS AGRO-INDUSTRIALES RICOS EN $CaCO_3$ Y WITHERITA ($BaCO_3$)

TESIS PARA OPTAR AL GRADO DE MAGISTER EN CIENCIAS, MENCIÓN GEOLOGÍA

ALFONSO TOMÁS LARRAGUIBEL QUIÑONES

PROFESOR GUÍA:
MANUEL CARABALLO MONGE

MIEMBROS DE LA COMISION:
LINDA DANIELE
BRIAN TOWNLEY CALLEJAS

SANTIAGO DE CHILE
2020

RESUMEN DE TESIS PARA OPTAR
AL GRADO DE: Magister
POR: Alfonso Tomás Larraguibel Quiñones
FECHA: 25/01/2020
PROFESOR GUÍA: Manuel Antonio Caraballo Monge

Optimización de tecnología DAS en laboratorio para retención de sulfato y metales de drenaje ácido de minas andinos utilizando residuos agro-industriales ricos en $CaCO_3$ y witherita ($BaCO_3$)

El sistema *Sustrato disperso alcalino* (DAS) es una tecnología pasiva de remediación robusta que ha mostrado altos niveles de rendimiento tratando drenajes ácidos mineros (AMD). Sin embargo, esta forma de abordar la remediación de aguas necesita mejorar respecto a su huella medioambiental, así como también el asegurar una completa remoción del sulfato en el agua por largos periodos de tiempo. El presente estudio mejora el uso de witherita ($BaCO_3$) como un material reactivo en tratamientos DAS, el cual induce retención de sulfato en el contexto de AMD andinos. Además, otros materiales carbonatados fueron probados como alternativas al actual uso de calcita. Se realizaron dos arreglos de experimentos con varios flujos (1.5-5.4 L/día), acides neta (202 y 404 mg/L de $CaCO_3$) y materiales reactivos (calcita, cáscara de huevo, conchillas marinas y witherita). Las conchillas marinas fueron validadas como reemplazantes al uso de calcita en etapas de $CaCO_3$-DAS y malaquita, un mineral presente en la retención de Cu en el agua, fue identificado por primera vez en este tipo de columnas. Las columnas de la etapa $BaCO_3$-DAS alcanzaron valores bajo los 500 mg/L de sulfato en la salida del sistema por los primeros 6 meses de funcionamiento, desde los 1234-2468 mg/L iniciales. Cálculos de escalamiento del presente estudio soportan la viabilidad de esta tecnología a escala de terreno, aunque se recomiendan estrategias para reducir los costos de la witherita.

Tabla de contenido

Índice de figuras

Índice de tablas

Capítulo 1

1.1 Motivación

Los drenajes ácidos mineros (AMD) son un problema ambiental muy relevante hoy en día, en particular para la industria minera. Estos se generan por la oxidación de sulfuros (y algunos sulfatos), que al entrar en contacto con agua liberan acidez, generando aguas con bajo pH y altos contenidos metálicos. En este trabajo de tesis de magister se plantea la implementación de un nuevo método de tratamiento pasivo adaptado a las condiciones chilenas. Este tratamiento se llama DAS (Dispersed alkaline substrate).

El trabajo de tesis consiste en el diseño y creación de un experimento a escala de laboratorio como un primer acercamiento del método DAS a las condiciones de aguas ácidas chilenas. La innovación respecto a investigaciones anteriores está relacionada principalmente a los materiales a utilizar: uso de conchillas marinas (en reemplazo de calcita) y uso de witherita (en reemplazo de periclasa), con la ventaja de retención de sulfato que brinda el uso de este ultimo material.

El análisis de resultados está enfocado en el comportamiento hidroquímico del sistema, en las fases minerales que retienen los metales y en las diferencias observadas respecto a flujo y carga metálica.

1.2 Estructura de la tesis

El presente estudio se separa en 4 capítulos. El presente capitulo introduce el tema de tesis, con sus principales objetivos e hipótesis de trabajo. El capítulo 2 corresponde a un manuscrito sometido a la revista Journal of Hazardous Materials, actualmente en revisión. Luego sigue el capítulo 3, el cual corresponde al material suplementario del manuscrito. Finalmente, el capítulo 4 corresponde a las conclusiones de la investigación.

1.3 Problemática ambiental de AMD

La sigla AMD significa “drenaje acido minero” (Acid Mine Drainage en inglés). No existe una definición estricta respecto a la composición que debe tener un agua para ser considerada un AMD, pero se puede definir como un agua con pH ácido en la cual hay una concentración importante de metales disueltos.

Existen 2 tipos de AMD: naturales y antropogénicos. Los AMD naturales (también llamados ARD, Acid Rock Drainage) son poco comunes (un ejemplo es el sector de Yerba Loca en Chile, Gutiérrez et al., 2015) pero el proceso por el cual se generan no es diferente al de un AMD antropogénico. Para que un agua sea considerada un AMD debe tener una alta concentración de protones disueltos y su generación ocurre por un proceso de oxidación de sulfuros o por disolución de sulfatos generadores de acidez. Es en este punto donde radica la diferencia entre los AMD naturales y antropogénicos. Un AMD natural es aquel en el cual la acidez liberada por los sulfuros ocurre sin la intervención de los humanos. Por otro lado, un AMD antropogénico se genera en un sector intervenido por el ser humano, en el cual se cambiaron las condiciones en las que se encontraban los sulfuros y debido a este cambio se activó su oxidación.

La generación de un AMD depende de la composición mineralógica del material. En este sentido, cada material posee un cierto potencial para producir acidez (PA) y un potencial para neutralizar la acidez (PN). Esto también se puede entender como la capacidad de un material para liberar protones (H^+) y para liberar hidróxido (OH^-). De forma simplificada, el PA está controlado por los sulfuros y metales presentes que puedan hidrolizarse, mientras que el PN está controlado por la presencia de silicatos y carbonatos. Otros minerales pueden generar reacciones de hidrolisis y neutralización acida al entrar en contacto con AMD, los cuales también pueden contribuir al PN. La disposición de los materiales, junto con la relación entre PA y PN será determinante para la posible formación de un AMD.

La liberación de acidez de los sulfuros ocurre cuando se conjugan 2 factores: condiciones oxidantes y presencia de agua. Debido a la actividad minera se retira material estéril para poder extraer el mineral de interés y muchas veces el material estéril tiene un porcentaje importante de sulfuros. Estos sulfuros, que se encontraban en condiciones no reactivas, debido a la actividad humana pasan a estar en condiciones oxidantes. Otra situación (entre otras) que puede provocar el cambio en las condiciones redox del sistema es el bombeo de agua que genera la presencia humana, la cual desencadena cambios en el nivel freático. Si llegan a cambiarse las condiciones redox del sistema, solo hace falta la presencia de agua para generar acidez y por ende un AMD.

A partir de esto, es evidente que en la mayoría de los depósitos de relaves y botaderos se puede generar AMD; estos se encuentran en la superficie en contacto con el aire y están expuestos a las precipitaciones. El agua de lluvia puede desencadenar la reacción con los sulfuros y estas aguas pueden escurrir a cursos de aguas cercanos, lo que puede generar un problema medioambiental importante tanto en la flora y fauna de la zona, así como también en las comunidades cercanas.

El análisis que se presenta a continuación considera a la pirita (FeS_2), el cual es el sulfuro generador de AMD más común en la mayoría de los yacimientos minerales.

La liberación de acidez a partir de pirita ocurre en 4 etapas, las cuales se presentan a continuación:

Ecuación 1: $FeS_2 + 3{,}5\ O_2 + H_2O \rightarrow Fe^{2+} + 2SO_4^{2-} + 2H^+$

Ecuación 2: $Fe^{2+} + 0{,}25\ O_2 + H^+ \rightarrow Fe^{3+} + 0{,}5H_2O$

Ecuación 3: $Fe^{3+} + 3H_2O \rightarrow Fe\ (OH)_{3(s)} + 3H^+$

Ecuación 4: $FeS_2 + 14Fe^{3+} + 8H_2O \rightarrow 15Fe^{2+} + 2SO_4^{2-} + 16H^+$

Cuando la pirita entra en contacto con oxígeno y agua (Ecuación 1) reacciona y libera hierro ferroso, 2 moles de sulfato y 2 moles de protones. Luego, ocurre la oxidación del ion ferroso a ion férrico (Ecuación 2), lo cual consume 1 mol de protones. Recapitulando, hasta esta etapa se genera solo 1 mol de protones.

Después de que se tiene el ion férrico, ocurre una reacción de hidrólisis (Ecuación 3) en la cual se genera un hidróxido de hierro y se liberan 3 moles de protones (4 en total, considerando el mol generando entre las etapas 1 y 2). Ya en esta etapa se puede apreciar un importante descenso en el pH del agua. Cabe destacar que según Dold (2003) "Cuando el pH baja a menos de 5, el proceso de oxidación del ferroso al férrico es muy lento" (p.31), es decir, la cinética de este proceso está controlada principalmente por la Ecuación 2. Esta cinética se puede ver influenciada por la presencia de bacterias quimiolitótrofas que catalizan la oxidación.

Finalmente, aun con ausencia de oxígeno, puede ocurrir la oxidación de la pirita directamente cuando hay presencia de ion férrico (Ecuación 4), generando una acidez muy importante. Cabe destacar que este último paso solo ocurre en condiciones ácidas cuando la solubilidad del hierro férrico lo permita. Se debe recalcar que, si este ion férrico se formó en el mismo sistema, se consumieron 14 protones en su producción (Ecuación 2) y por ende el saldo de acidez no es tan alto como aparenta ser. Lo relevante ocurre cuando el ion férrico que reacciona con la pirita proviene de otro lugar (como lo puede ser un afluente a un río principal); en este caso la cantidad de acidez producida es 8 veces mayor y la bajada de pH es muy pronunciada.

El principal problema que tiene la generación de acidez no radica en las altas concentraciones de protones en sí mismo, sino en las altas concentraciones de metales que conlleva una disminución del pH. La solubilidad de los metales está fuertemente afectada por el pH del agua, siendo esta alta en pH extremos, es decir, la solubilidad de metales es considerable en pH ácidos y extremadamente alcalinos. En general, la precipitación de metales al aumentar el pH ocurre en forma de hidróxidos, los cuales pueden generar diversos problemas en la forma de tratar las aguas (especialmente en los métodos pasivos de tratamiento).

El pH exacto de precipitación de los metales todavía es un tema de estudio, pero se manejan rangos en los cuales se sabe que el metal ya no es soluble. El aluminio precipita cuando el pH es sobre 5 y vuelve a disolverse en valores de pH superiores a 9, mientras que el hierro precipita a pH aproximadamente de 3,5. El manganeso requiere pH mayores para su precipitación (9-10) y por ende tiende a ser problemático debido a que muchos metales vuelven a disolverse a estos pH alcalinos.

La mayoría de los metales trivalentes ya no son solubles en pH neutros, mientras que los divalentes tienden a precipitar en pH más altos (cercanos a 8-9). En base a esto, para que la purificación de agua sea lo más eficiente posible, es ideal que el pH del agua termine al menos en 8 y ojalá que posteriormente se remueva el manganeso (de ser importante su concentración en el AMD).

1.4 Sulfato en AMD

Como se vió anteriormente en la Ecuacion 1, el proceso de generacion de acidez de la pirita tambien libera sulfato. Para entender el comportamiento del sulfato en el agua, es necesario entender la disposicion de la molecula que lo compone (Figura 1). Como se puede ver, 2 de los 4 atomos de oxigeno forman un enlace doble con el azufre central, mietras que otros 2 solo poseen un enlace simple. Esto significa que en este estado el azufre posee una valencia de 6+, resultando en una molecula con 2 electrones libres. Dicho de otra forma, S^{6+} es un cation con alto potencial iónico (carga ion/radio ion) y por ende tenderá a formar oxocomplejos (en este caso, la molecula de sulfato), permaneciendo en solución. Tambien es posible que genere enlaces con metales como el Fe, Ca, Mg, entre muchos otros.

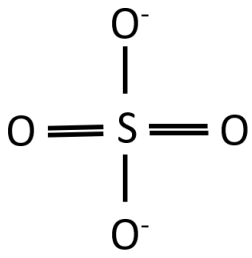

Figure 1: Molécula de sulfato (SO_4^{2-})

La presencia de sulfato en el agua se puede dar por intervención humana directa (desechos industriales, fertilizantes, etc), de forma natural (disolución de sales al entrar en contacto con agua) o por intervención humana de forma indirecta. Es en este último punto donde se centra la problemática de sulfato en AMD.

La presencia de sulfato en el agua es levemente perjudicial para la vida humana. En general, los efectos adversos se encuentran con concentraciones de sulfato sobre 750mg/L aproximadamente. El mayor punto de interés se centra en el consumo de sulfato por niños pequeños, los cuales son más propensos a sufrir los efectos adversos. Respecto a los animales, el sulfato se considera toxico en concentraciones elevadas (sobre 2500-3000mg/L). A continuación, se presenta una lista con algunos de los daños que puede generar su presencia en el agua consumida:

-Deshidratación en humanos (Fingl, 1980)

-Diarrea y problemas intestinales (US EPA, 1999a,b) (Chien et al, 1968)

-Efecto laxante (Esteban et al, 1997) (US EPA, 1999b)

-Toxicidad en ganado (Smith 1980)

Además, la presencia de sulfato en el agua genera problemas de olor y sabor en el agua (National academy of sciences, 1977). Por último, la presencia de sulfato también puede tener efectos corrosivos en tuberías en sistemas de disposición de aguas (Larson 1971). En el caso de Chile, la ley de descarga DS90 tiene como limite 1000mg/L de sulfato. Por otro lado, las leyes NCh 1333 y NCh 409/1 tienen límites de 500 y 250mg/L respectivamente.

La presencia de sulfato en AMD es un problema importante y muchas veces una limitante al intentar cumplir con las diversas normas de calidad de agua. Esto ocurre debido a que la mayoría de los procesos de tratamiento de AMD aumentan el pH del agua para así retener metales, proceso que muchas veces no retiene sulfato (o lo hace en cantidades menores a las deseadas).

Al hablar sobre tipos de tratamientos de AMD hay que tener en consideración que existen 2 grandes categorías: los métodos activos y los métodos pasivos. Los métodos activos son tipos de tratamiento con un input energético que les permite ser más eficientes, más controlados y a su vez más costosos y con mayor impacto medioambiental (Figura 2). Por otro lado, los métodos pasivos tienen un input energético bajo (o nulo), tienden a estar más limitados y a ser más amigables con el medio ambiente. Mas allá de si el sistema es activo o pasivo, la forma de abordar el problema también genera una distinción. En este sentido, el tipo de tratamiento puede ser físico, biológico o químico.

Figure 2: Planta HDS, utilizando maquinaria y un input de energía importante. Fuente: Taylor et al, 2005

Existen métodos activos capaces de retener el sulfato en el agua. Uno de ellos es el método HDS, el cual ataca el problema a partir de la generación de sulfato de calcio (Aubé et al, 2018). Por otro lado, existen alternativas más ecológicas como el utilizar bacterias sulfato reductoras (Liu 2017), sistema efectivo, pero poco práctico al considerar sus limitaciones respecto a agua de entrada y altos tiempos de retención.

1.5 Tecnología DAS

Un ejemplo de cómo tratar AMD ocurre en la península ibérica en España. En este lugar se encuentra una gran concentración de sulfuros, denominada faja pirítica ibérica. En esta provincia la industria minera se desarrolló fuertemente y genero un problema de AMD importante. En la Figura 3 se pueden ver los niveles de acidez que son capaces de tratar los métodos pasivos más utilizados, frente a los niveles que presenta esta zona.

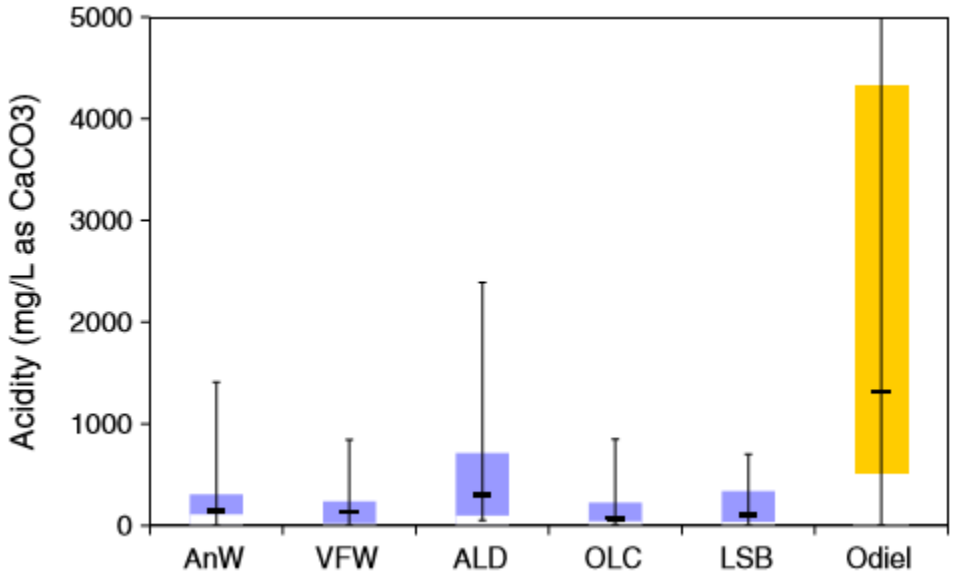

Figure 3: Comparación de acidez neta (percentiles 25%, 75% y promedio) de aguas tratadas con métodos pasivos convencionales (80 muestras) y la acidez de la cuenca Odiel (ubicada en la península ibérica, 245 muestras). AnW anaerobic wetlands, VFW vertical flow wetlands (RAPS), ALD Anoxic limestone drains, OLC oxic limestone channels, LSB limestone leach beds. Fuente: Ayora et al (2013).

La purificación de las aguas de la zona tenía problemas no solo en las altas concentraciones de metales en los AMD, sino también en los costos asociados al tratamiento; muchos de los AMD se generaban en minas fuera de producción y por ende los costos de mantención no podían ser elevados. En base a esto, la implementación de un sistema de tratamiento pasivo de AMD era el ideal para poder no solo mantener un modelo sustentable económicamente, sino también dar un ejemplo medioambiental de cómo solucionar una problemática de este estilo.

A través de los años se implementaron varios sistemas pasivos de tratamiento de AMD. Sin embargo, estos presentaron problemas de pasivación y perdida rápida de conductividad hidráulica, problemas comunes en tratamientos pasivos que reducen su vida útil. A partir de ello, se desarrolló e implemento un nuevo método para tratar los AMD de la faja pirítica ibérica.

Uno de los problemas principales de los tratamientos pasivos que utilizan caliza radica en el tamaño de grano a utilizar. Por un lado, es deseable que el tamaño de grano sea fino y de esta forma aumentar la eficiencia del sistema al aumentar el área de superficie entre la calcita y el AMD. Por otro lado, la permeabilidad que posee un sistema con material de grano fino es muy baja y no permite tratar cantidades importantes de agua. En base a esto último, un tamaño de grano más grueso le entrega una conductividad hidráulica al sistema que permite un tratamiento eficiente.

A partir de esta disyuntiva surge el método DAS, el cual considera este problema del tamaño de grano, planteando una solución eficiente y ecológica. El método consiste en un sustrato compuesto por 2 materiales: Un material inerte y un material reactivo. El material inerte es un material que no reacciona con el AMD, es de tamaño grueso (le entrega la permeabilidad deseada al sistema) e idealmente es un material de desecho de alguna otra industria. El material reactivo será un material que tenga la capacidad de neutralizar la acidez del AMD y tendrá un grano fino que permite un área de superficie alta (y por ende una mayor eficiencia). Esto también soluciona parcialmente el problema del precipitado de hidróxidos; el mayor espacio entre granos permite que los precipitados no tapen el sistema tan rápidamente.

Hasta ahora, la forma de tratamiento se separa en 2 etapas. La primera de ellas utiliza calcita como material reactivo, subiendo el pH hasta valores neutros y reteniendo metales trivalentes. Luego, en una segunda etapa se utiliza periclasa para subir aun mas el pH y generar retención de metales divalentes. Sin embargo, ninguno de los 2 procesos es capaz de reducir las concentraciones de sulfato a niveles aceptables por las normas nacionales. Existe un estudio reciente (Torres et al, 2018) en Sudáfrica que utiliza witherita como material reactivo para retener sulfato en el contexto de la tecnología DAS. Sin embargo, el tiempo de funcionamiento de las pruebas realizadas en este estudio son de alrededor de 40 días, lo cual es insuficiente par poder validar el uso del material como una solución al problema.

1.6 Contexto chileno

Ya existen investigaciones (Caraballo et al 2011, Ayora et al 2013) que prueban que el método DAS es efectivo en la remoción de metales de AMD provenientes de la faja pirítica ibérica. Sin embargo, existen importantes diferencias entre esta zona y los yacimientos en Chile que no permiten asegurar que una implementación del método DAS en nuestro país sea eficiente. Estas diferencias radican en 2 ejes centrales: magnitudes de flujos a tratar y elementos (y sus respectivas concentraciones) contenidos en el AMD.

Los flujos de aguas a tratar en Chile son muy diversos, ya que existe minería a diferentes escalas y en diferentes zonas que generan una variabilidad muy importante. En contraste, los flujos de AMD de la faja pirítica ibérica tienden a ser menores y en rangos más acotados. Es por esto que es importante probar el sistema DAS para flujos diferentes y así probar la eficiencia del sistema en diferentes condiciones más cercanas a la realidad de Chile. Además, hay diferencias en el clima y humedad ambiental que eventualmente pueden afectar a los procesos evaporíticos del sistema ya en terreno.

Respecto a los elementos a purificar, también existen diferencias importantes. Estas diferencias están evidentemente ligadas a la mineralogía de los yacimientos de cada zona. Para el caso de la faja pirítica ibérica, dominan los depósitos volcánicos de sulfuros masivos (VMS) con cantidades importantes de sulfuros hierro, cobre, zinc y plomo, así como algo de plata y oro (Leistel et al 1997). En contraste en Chile dominan los yacimientos tipo pórfido cuprífero, junto con yacimientos epitermales, IOCG y estratoligados. La mineralogía de este tipo de yacimientos es diversa, incluyendo minerales de mena como calcopirita, alunita, bornita, molibdenita y covelina, además de minerales de ganga como hematita, pirita, cuarzo, entre muchos otros. La principal diferencia con la faja pirítica ibérica radica en que en Chile los AMD poseen concentraciones en espectro mucho menores, especialmente en elementos como zinc, plomo e hierro.

Por estas razones surge la interrogante de la eficiencia del método DAS en Chile, país que contiene AMD con concentraciones de metales mucho menores y con una variabilidad de elementos más diversa. Por otro lado, es interesante poder buscar un reemplazo de la calcita como material reactivo. Esto debido a que el método se puede hacer aún más amigable con el medioambiente si se utilizan otros materiales locales para la purificación del agua.

1.7 Objetivos

1.7.1 Hipótesis de trabajo

La sustitución de calcita por un residuo carbonatado y el uso de un paso de tratamiento que incluya witherita ($BaCO_3$) permitirá el diseño de un sistema de tratamiento tipo DAS más sustentable y con una significativa retirada de sulfato por largos períodos de tiempo.

1.7.2 Objetivo general

Probar la viabilidad de uso de materiales reactivos alternativos en el sistema de tratamiento pasivo DAS. Uso de conchillas marinas en reemplazo de calcita y uso de witherita en reemplazo de periclasa. Todo esto enfocado desde un punto de vista mineralógico e hidroquímico.

1.7.3 Objetivos específicos

-Ampliar la aplicabilidad del método DAS, respecto a flujo y carga metálica

-Analizar comportamiento de columnas con witherita, a través de muestras de agua, análisis DRX y SEM.

-Comprobar comportamientos y tendencias de la primera etapa de tratamiento, sometida a condiciones de carga y flujo chilenas.

1.8 Diseño experimental

En base a lo planteado anteriormente en este capítulo, se decidió realizar experimentos en columnas de laboratorio que sean capaces de entregar información y por ende una eventual viabilidad a materiales reactivos alternativos a los ya conocidos en el tratamiento DAS, todo esto en el contexto de inputs de agua con características locales. Para ello, se realizaron 2 experimentos:

$CaCO_3$-DAS: Experimento llamado ¨DAS carbonatado¨, el cual consiste en 4 columnas en paralelo, cada una con un material reactivo carbonatado distinto y manteniendo condiciones de input de AMD y flujo de entrada constantes. El experimento tiene como fin el probar si efectivamente otros materiales carbonatados de desecho son efectivos en la subida de pH y retención de metales trivalentes.

$BaCO_3$-DAS: Este experimento tiene como finalidad generar retención de sulfato en el sistema. Para ello, se utiliza witherita como material reactivo (en reemplazo de periclasa, material usado hasta ahora en experiencias anteriores). Además de utilizar un nuevo material reactivo, se varían condiciones de flujo y acides neta de entrada, para robustecer los parámetros de funcionamiento del sistema.

Cabe destacar que los caudales utilizados en estos experimentos (los cuales se detallan en los capítulos 2 y 3, figuras 4, 9 y 10, junto con las tablas 2 y 5) están basados en experiencias previas, en donde el factor relevante pasa a ser la carga metálica por superficie de material. Teniendo las dimensiones de la columna y la carga metálica particular del drenaje acido, se utiliza un caudal adecuado para que el experimento funcione de forma adecuada.

Capítulo 2

Optimization of DAS technology to remove sulfate and metals from Andean AMDs using $CaCO_3$-rich residues from agri-food industries and witherite ($BaCO_3$)

Alfonso Larraguibel[a,b], Alvaro Navarrete-Calvo[a,b], Sebastián García[b,c], Manuel A. Caraballo[b,c]

[a]Geology Department, University of Chile, Plaza Ercilla 803, Santiago, Chile

[b]Advanced Mining Technology Center, University of Chile, Avda. Tupper 2007, 8370451 Santiago, Chile

[c]Mining Engineering Department, University of Chile, Avda. Tupper 2069, Santiago, Chile.

Highlights:

- Sea- and egg-shells proven as sustainable alternatives to calcite on DAS systems
- Water high alkalinity and low Al/Cu ratios generates malachite in $CaCO_3$-DAS columns
- Long-term removal of different loads of sulfate was achieved using $BaCO_3$-DAS columns
- $BaCO_3$-DAS upscaling to full scale treatment is feasible under a circular economy strategy

Abstract:

Dispersed alkaline substrate (DAS) is a matured passive remediation technology that has shown very high performances treating acid mine drainages (AMD). However, this remediation approach needs to improve its environmental footprint as well as to ensure almost complete water sulfate removals for longs periods of time. The present study improves the use of witherite ($BaCO_3$) as a reagent on DAS-type treatments to induce high water sulphate removals in the context of Andean AMD. Also more sustainable $CaCO_3$ materials were tested as alternatives to the current use of limestone. Two sets of column experiments were developed with various flow rates (1.5-5.4 L/day), net acidities (202 and 404 mg/L of $CaCO_3$) and reactive agents (calcite, eggshells, seashells and witherite). Seashells were validated as a perfect limestone substitutes on the $CaCO_3$-DAS stages and malachite, as a mineral phase actively involved in Cu water removal, was observed for the first time within these columns. The $BaCO_3$-DAS columns achieved values under 500 mg/L of sulfate at the output of the system for up to 6 months. Upscaling calculations of the present results support the feasibility of using this technology at a full field scale, although some strategies to reduce witherite costs are recommended.

Keywords: dispersed alkaline substrate, malachite, acid mine drainage, seashells, passive treatment system.

2.1 INTRODUCTION

Acid mine drainage (AMD) is a specific type of water pollution resulting from its interaction with sulfide minerals (mainly pyrite) at oxidizing environments [1]. As a result, this environmental problem is ubiquitously present around the world in mined and un-mined sulfide rich rocks [2]. These drainages are characterized by high metals and sulfate concentrations and low pHs, making them extremely harmful for the environment [3,4,5].

Because of the severity and widespread distribution of this water pollution around the world, a substantial amount of different remediation approaches have been generated during the last three decades [6,7,8]. The most frequently used treatments to remediate high flow rates of AMD are characterized by an intensive use of energy to power the multiple mobile mechanical parts and electronical components of the industrial treatment plants [9,10], and for this very reason this approach is typically referred as active treatments. The particular design of an active treatment depends on both the specific water pollution to be treated and the water quality to be achieved at the output of the system. Therefore, a variety of treatments units (e.g., neutralizing reactors, softening reactors, filtration and/or reverse osmosis) are frequently connected in series to achieve the desired water quality [9]. However, a common denominator of most active treatments is the use of a neutralizing step, with lime ($Ca(OH)_2$) as the most frequent chemical reagent, to raise water pH and induce the precipitation of metals. Active treatments commonly require high maintenance, high chemical reagents and energy consumptions and highly specialized operators, resulting in significant capital and operational (CAPEX and OPEX) expenditures. Nowadays, they are used primarily in active mine sites [9].

On the other hand, there are the so-called passive treatments that use a different approach to treat AMD with a minimal or none use of electrical energy. Those treatment technologies are designed to favor the gravitational flow of the AMD through one or more different layers and/or steps designed to remove metals and/or sulfate and increase water pH at the same time. They commonly require important expenditures in the initial construction phase (land removal and civil-engineering-type construction) but a low maintenance, no energy consumptions and the absence of highly specialized operators during the operation of the plant, (high CAPEX but low OPEX); resulting in cheaper and more environmentally friendly options if compared with active treatments [3,9,11]. However, as a downside, they use to have some limitations regarding the metals and sulfate concentrations of the inflowing AMD and substantial limitations considering AMD inflow rates (i.e., inflow rates are typically lower than 50 L/s, depending on the water chemistry) [7,8,12]. Passive treatments can also be sub-divided in two big categories: biogeochemical- (e.g., vertical flow reactors or aerobic and anaerobic wetlands) or geochemical-based systems (e.g., anoxic limestone drainage or limestone permeable barriers), and different hybrid options combining both of them [3,13]. Passive treatments systems may face several specific problems depending on their individual design and geochemical or biogeochemical approach. Notwithstanding, most of these treatments frequently suffer from two common problems: clogging (progressively reducing the flowrate that the system can receive) and reactive material passivation (the reactive material gets isolated from the AMD by a cover of precipitates and loses its neutralizing capacity) [8,14,15]. All these considerations make passive treatments a more suitable remediation option for closed or abandoned mine sites or as a compliment of other active treatments in active mine sites.

On an effort to overcome the frequent clogging and passivation issues observed on most traditional AMD passive treatment systems, the concept of Dispersed Alkaline Substrate (DAS) was first introduced in 2006 [16,17]. DAS consists on a mixture of a coarse-grained inert material (to prevent clogging problems by the generation of a high porosity substrate) and a fine-grained reactive material (to minimize passivation by enhancing the reactive material dissolution rate) [18]. This treatment technology has been optimized and improved for more than a decade using mostly AMDs from the Iberian Pyrite Belt (IPB, SW Spain) [8,19,20,21,22]. Those polluted waters are characterized by very high to extreme metal and sulfate concentrations and low to very low pH values (Table 1, input waters). Historical operational conditions and performances of DAS-type treatment systems (i.e., laboratory column experiments, pilot plants and field full scale treatment systems) has been summarized in Table 1 in order to identify the strengths and weakness of this mature technology. All laboratory and field experiments until 2018 were based on different combinations of operational units using limestone sand ($CaCO_3$) and/or periclase dust (MgO) as reagents to increase water pH. Typically, limestone dissolution increases water pH around 6 and induces the removal of trivalent metals by the precipitation of schwertmannite ($Fe_8O_8(OH)_6SO_4 * 5H_2O$) and hydrobasaluminite ($Al_4(SO_4)(OH)_{10} * 36H_2O$); whereas periclase dissolution generates water pHs higher than 8.5 inducing the precipitation of divalent metals like Zn^{2+}, Mn^{2+}, Ni^{2+}, Cd^{2+} or Co^{2+} (Table 1). Detailed explanations on the geochemical and mineralogical processes governing these trivalent and divalent metals removal as well as some other metals and metaloids adsorption and/or co-precipitation can be found in the substantial existing bibliography on this topic (Table 1).

Input and output net acidity (as mg/L of $CaCO_3$) can be used to evaluate the system remediation performance, since this parameter is calculated taking into consideration the five most relevant elements controlling the AMDs hydrochemistry (i.e., Al, Cu, Fe, Zn and Mn) as well as water pH and alkalinity values. All limestone- and/or periclase-based DAS treatment systems achieved very good acidity removals, being able to reduce water net acidities from values in the range of 1,500-5,000 mg/L as $CaCO_3$ to net acidities at the systems outputs on the range of 0 to 900 mg/L as $CaCO_3$ (depending on the specific experiment performance, Table 1). It is important to highlight that the most recent experiences were able to optimize the system performance and obtain net acidity values at the output of the systems close to 0 mg/L as $CaCO_3$ (i.e., experiences from 2012 to 2018, Table 1). However, all those treatments were unable to significantly reduce sulfate water concentrations, achieving sulfate removals on the range of 0% to 40% comparing input and output concentrations (Table 1).

Table 1: Historical operational conditions and performance of DAS-type treatment systems

Location			Monte Romero	Monte Romero	Monte Romero	Shillbottle	Mina Esperanza	Monte Romero	Monte Romero	Almagrera	Poderosa Mine	Mina Concepcion
Experiment Scale			Lab columns	Pilot plant	Pilot plant	Lab columns	Field full scale	Field Pilot plant	Lab columns	Lab columns	Lab columns	Field full scale
Input mean values	pH		2.8	3.3	3.08	3.9	2.65	3.58	2.7	2.6	2.4	2.7
	Al		106	75	117	200	147	80	128	251	532	119
	Fe		250	315	358	5	900	260	161	744	1052	286
	Zn	(mg/L)	365	310	388	102	26	350	431	976	0.06	20
	Mn		22	20	19	77	5	13.5	18	467	0.003	N/A
	Cu		3.3	1.5	10	N/A	18	2.7	7	165	0.096	N/A
	SO_4^{2-}		3510	3200	3640	N/A	3900	3430	3500	11700	7532	N/A
	Net Acidity	(mg/L of $CaCO_3$)	1727	1500	2450	1500	2500	1609	1800	5000	5000	1300
Output mean values	pH		6.5	6	5.9	9.5	5.7	9.8	6.8	7.5	7.6	7.2
	Al		2	5.25	3.4	50	2	<0.2	0.26	0	0.1	dl
	Fe		2	237	83	0	600	<0.2	0	0	0.08	25
	Zn	(mg/L)	350	294	279	20	15	<0.05	7.84	1.7	0.00004	dl
	Mn		22	20	17	45	3	<0.2	3.38	14.5	0.000898	N/A
	Cu		0.5	0.015	0.2	N/A	0.5	<0.005	0.03	0.05	0.00008	N/A
	SO_4^{2-}		3500	3200	3500	N/A	3500	2800	3600	14400	22	N/A
	Net Acidity	(mg/L of $CaCO_3$)	500	630	632	400	900	0	20	30	0	50
Flow rate	(L/day)		0.14-1			1.5			1	1	0.4	
	(L/min)			1	1			1				
	(L/s)						0.5					0.8
Residence Time	(hours)		31-168	24	24 (Lim), 10 (Per)	12	54	36 (Lim), 12 (Per)	17	17	30	70-160
Duration	(months)		16	11	9	3	20	6	4.5	4.5	1.5	12
Reactive materials			Lim.	Lim.	Lim. & Per.	Per.	Lim.	Lim. & Per.	Lim. & Per.	Lim. & Per.	Lim. & With.	Lim. & Per.
References			Rotting et al., 2008a	Rotting et al., 2008b	Caraballo et al., 2009	Caraballo et al., 2010	Caraballo et al., 2011	Macias et al., 2012	Ayora et al., 2016	Ayora et al., 2016	Torres et al., 2018	Martinez et al., 2018

All location are in the Iberian Pyrite Belt, SW Spain except for Shillbottle that is in NE England

Lim. = Limestone ($CaCO_3$); Per. = Periclase (MgO); With. = Witherite ($BaCO_3$)

N/A: Not Analyzed or Not Available, dl: Detection Limit

Net acidity calculated as follows when not directly available: $50.045(3C_{Al}+2C_{Fe}+2C_{Mn}+2C_{Zn}+2C_{Cu}+10^{-pH})$-alk. C_X: molar concentrations. Modified from Rotting 2008a to consider Cu.

Sulfate upper limit concentrations in water quality guidelines for irrigation or for drinking depend on each country environmental legislation but typical values are on the ranges of 150-1000 mg/L and 250-500 mg/L, respectively [26]; whereas AMD waters, at the IPB, treated by limestone- or periclase-based DAS treatments systematically show water sulfate concentrations higher than 3,000 mg/L (Table 1).

To tackle the sulfate problem, witherite ($BaCO_3$) was recently tested at laboratory scale as a possible new alkaline reagent substituting limestone or periclase [22]. Witherite dissolution induces sulfate precipitation as barite ($BaSO_4$) according to the following reaction:

$$Ca^{2+}_{(aq)} + SO_4^{2-}_{(aq)} + BaCO_{3(s)} \rightarrow BaSO_{4(s)} + CaCO_{3(s)} \quad (1)$$

Witherite dissolution also increase AMD pH to values around 7 or 8 with the concomitant precipitation of all trivalent metals in solution as well as some divalent metals too [22]. This recent experiment showed promising results, inducing almost complete sulfate removal and complete net acidity removal (Table 1). However, this exploratory experiment only last one month and a half, used a very low inflow rate (0.4 L/day) and was tested at extreme net acidity conditions (5,000 mg/L as $CaCO_3$).

In addition, a recent life cycle assessment study performed on the field full scale DAS passive treatment at Mina Concepción, SW Spain [27], revealed that the use of limestone from a quarry located far from the treatment system have a substantial impact on its carbon and ecological footprint. On this respect, the reuse of alternative by-product or residues (instead of mining raw materials) should be encouraged. Also, it is important to consider that all experiments, but the one in 2010 using the AMD from Shillbottle (UK), were performed using AMDs with very high to extreme metal and sulfate contents and the applicability and performance of this technology at lower metal and sulfate concentrations have not been properly studied. These AMDs with lower metal and sulfate concentrations are very typical in many mining regions (e.g., porphyry copper deposits, coal deposits, etc.) around the world that could benefit from the implementation of an optimized DAS technology.

The main scopes of the present study are: 1) to investigate different options of more sustainable alkaline materials to replace limestone from quarries, 2) to optimize the best sequence of DAS passive treatment steps to treat AMDs with low to medium acidity and sulfate contents, and 3) to evaluate the use of witherite to remove variable sulfate loads during long periods of treatments (i.e., higher than half a year).

2.2 MATERIALS AND METHODS

2.2.1 Chilean and Argentinian AMDs as possible low acidity AMD proxies

As mentioned on the introduction section, DAS passive treatment technology has been successfully used to remove di- and tri-valent cations from highly polluted AMDs, but its performance on less concentrated AMDs is still pending. Although an efficient and positive applicability of this technology to less polluted waters can be anticipated, its specific implementation is not straightforward because a few operational parameters must be optimized and its working ranges defined (i.e., residence time, flowrate that can be treated, metal removal efficiency and duration of the reactive material prior to its passivation or its total consumption). On this respect, it was decided to perform an exploratory bibliographic study of reported AMD waters in the Andes (mostly in Chile and Argentina) to obtain a broad picture of the type of low to medium AMD polluted waters developed on this geological setting. In this part of the Andes, the mine industry is heavily focused on Cu extraction and the most common mineral deposits (and residues) include porphyry copper, iron oxide copper ore deposits (IOCG) and/or iron oxide apatite deposits (IOA), and Stratabound [28][29].

In an attempt to characterize AMD flows in Chilean and Argentinean Andes, 296 samples analyses from 32 different field sites were gathered on a database (Table S1, Supplementary Information). The statistical distribution of the samples and the main statistics are shown in Table S1. The original synthetic AMD (AMD 1x, Figure 4) used in the lab experiments was created to reproduce the water chemistry of a real sample with a net acidity value close to percentile 75 of the generated database (line 171 highlighted on green on Table S1, Supplementary Information). By doubling the concentrations of the original synthetic AMD, (AMD 2x, Figure 4) a net acidity of 404 mg/L as $CaCO_3$ was obtained. This new synthetic AMD has a net acidity value close to percentile 90 of the created database of Andean AMDs from Chile and Argentina. Therefore, the present lab experiments will potentially have direct application to most AMDs in our database.

2.2.2 Experimental design

To achieve the main goals of the present study, a sequence of two different sets of laboratory experiments were designed and implemented ($CaCO_3$-DAS and $CaCO_3$-DAS+$BaCO_3$-DAS Experiments in Figure 4).

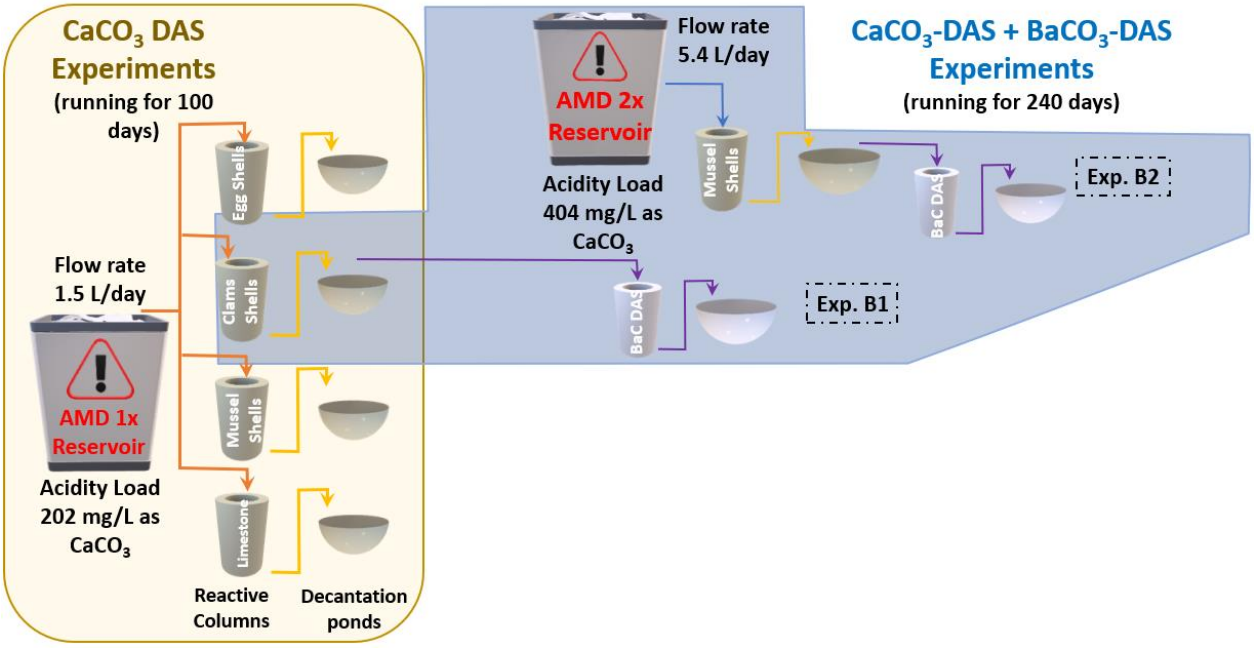

Figure 4: Experimental design showing the three different experimental setups implemented. The composition of the AMD (mark as x on the graphic) is shown in detail on Table 5 (Chapter 3). This composition is multiplied by 2 to generate the second AMD reservoir.

During the first experiment, four different calcium carbonate ($CaCO_3$) reagents were tested to evaluate the possible substitution of commercial limestone (traditionally used in all previous field and laboratory DAS studies and obtained from the closest available quarries) by a more sustainable material (i.e., an industrial residue that could be reused and re-conceived as a by-product rather than as a residue). At the same time, the DAS system performance treating an Andean AMD with moderate metals and sulfate concentrations will be tested. All the columns were fed for 100 days using the synthetic AMD previously mentioned (Table 5, Chapter 3) and a flow rate of 1.5 L/day. All columns had 50% porosity and a water residence time of 48h. Reactive material to wood shavings volumetric ratio was 1 to 4 within the calcite-DAS and clams shells-DAS columns and 1 to 5 within the mussels shells-DAS and eggs shells-DAS columns. Notice that all the columns on this and the following experiments are followed by a decantation/reaction pond, which are designed to ensure the needed time for the water to equilibrate and complete the mineral precipitation reactions involved in the water treatment. Additional details about the columns and decantation ponds setups and construction can be found in Chapter 3 (Fig. 9 and 10).

The second experiment was focused on the assessment of the different operational parameters affecting sulfate removal using $BaCO_3$-DAS columns on long term experiments. On this respect, AMDs with two different concentrations (x and 2x, Figure 4 and Table 5) were fed to two different columns using two different inflow rates (Table 2). As a result, the effect on $BaCO_3$-DAS columns performance of two different sulfate loads (i.e., 1.9 and 13.3 g/day) was evaluated. This last experiment was maintained for 8 months to clearly evaluate the system performance during long periods of time.

Table 2: Main operational conditions of the different columns setups in the experiments including a $BaCO_3$-DAS step

Table 2. Main operational conditions of the different columns setups in the experiments including a $BaCO_3$-DAS step.

	Net acidity (mg/L of $CaCO_3$)*	SO_4^{2-} (mg/L)	Flow rate (L/day)	SO_4^{2-} load (g/day)	Acid load#	Columns residence time (h)	Total duration (months)	Columns reactive materials	Reactive/inert material proportions
Experiment B.1	202	1234	1.5	1.9	53.86	48	8§	Clams shells →Witherite	16/84 (v/v) 1/1 (w/w)
Experiment B.2	404	2468	5.4	13.3	387.84	13.5	8	Mussels shells →Witherite	20/80 (v/v) 2/1 (w/w)

* Net Acidity=$50.045(3C_{Al}+2C_{Fe}+2C_{Mn}+2C_{Zn}+2C_{Cu}+10^{-pH})$-alk. C_X: molar concentrations. Modified from Rotting 2008a to consider Cu.

Calculated as (flow rate*net acidity)/(1000*horizontal treatment area).

§ It is important to keep in mind that the CaCO3-DAS columns have an extra 100 days in these experiments.

2.2.3 Sampling and analysis

Water samples were collected (using lateral sampling ports as well as input and output waters) on a monthly base (or shorter) during the operation time of the different experiments. Filtered samples (filter pore size of 45 µm) were acidified with HNO_3 until reaching a pH value close to 1 and stored at the refrigerator at 4°C until analysis. The chemical analyses were performed by ICP-MS and ICP-OES at external analytical company (i.e., Bureau Veritas/Acmelabs) using a commercial analytical package (i.e., ICP-MS S0200 analysis for natural waters). The detection limits achieved are lower than the regulatory limits proposed by the World Health Organization (WHO) [30] and the US Environmental Protection Agency (USEPA) [31]. Specific values for these limits are shown in Figure 11 (Chapter 3).

Physicochemical parameters such as pH, Eh, OD and EC were measured using a Thermo Orion Star A329 portable meter, with the following electrodes: For pH Orion 8107UMMD, for ORP measurements Orion 9179BN, for EC Orion 013010MD and for OD Orion 087003. The calibrations solutions used were: Orion pH buffers 910104 (pH 4.01), 910107 (pH 7), 910110 (pH 10.01), ORP standard Orion 967961, EC standards Orion 011007 and Orion 011006. All electrodes were properly calibrated before each measurement campaign.

Solid samples were taken at the end of each experiment, every 4 cm in the upper segment of the substrate and every 6 cm afterwards. An additional sample for each column was taken on the surface (5 mm). The samples were oven-dried (Oven Memmert UN-110) at 30°C for 3-4 days, milled using an agathe mortar and pistil and finally sieved under 75 µm.

The semi-quantitative mineralogical analyses of the solid samples were obtained using powder X-ray diffraction (XRD) of randomly oriented samples on Bruker D5005 X-ray diffractometer with CuKα radiation. Diffractometer settings were: 40 kV, 30 mA, and a scan range of 10–63° 2θ, 0.02° 2θ step size, and 5s counting time per step. The obtained diffractograms were analyzed using the software XPowderX® and PDF2 database (Figure 6 and Figures 12-13 on Chapter 3). Fluorite was added to the samples as internal standard to correct any possible drifting of the diffractograms and to improve the calculations of the minerals concentrations. More detail about the specific analysis procedure are offered in Chapter 3.

Electron microscopy images and chemical analyses by energy dispersive spectroscopy were obtained with a SEM-EDS FEI Quanta 250. Samples were analyzed using three different detectors: ETD (Everhart Thornley detector), BSED (Backscattered electro detector) and EDX (Energy dispersive x-ray). The instrument was operated using a Voltage range of 10 kv to 30 kv. The images were process using the Quanta 250 interface whereas the EDX analysis were studied using the software INCA®.

2.2.4 Hydrogeochemical Model

The geochemical model was implemented using the open source geochemical software (PHREEQC) which is a powerful reaction based software with a long tradition in the fields of mining and environmental engineering studies [30]. Detailed explanations of the conceptual geochemical models used as well as the specific chemical reactions, kinetic equations, mineral equilibrium phases, and cells dynamic characteristics during the reactive transport model are offered in Chapter 3 (Tables 6, 7 and 8).

2.3 Results and Discussions

2.3.1 Assessment of $CaCO_3$ rich residues from agri-food industries treating an Andean AMD with intermediate metals and sulfate concentrations

As previously mentioned, the first experiment was designed to evaluate: 1) the possible substitution of commercial limestone by a more sustainable material and, 2) the DAS system performance when treating an Andean AMD with moderate metals and sulfate concentrations. Taking into consideration the singularities of the Chilean geography and industrial matrix, it was decided to test two different types of sea shells (clams and mussels shells) as well as eggshells. These materials are very common residues from the Chilean agri-food industries that can be easily found in big amounts on various locations along the country.

As can be observed in Table 3 all experiments showed a very similar performance, achieving almost complete removal of all trivalent metals (i.e., Fe and Al) as well as very high removals for Cu and Zn. The concentrations achieved by these four elements are under the limits proposed by the World Health Organization (WHO) [31] and the US Environmental Protection Agency (USEPA) [32]. On the other hand, no significant removal of Mn and sulfate was achieved and their concentrations in the outflowing waters are over the limits proposed by the WHO and the USEPA. Regarding final water pH only small differences were observed, ranging all the experiments between 6.8 and 7.3. So, if the performance of each different reagent is evaluated in terms of metal removal and pH increase, all of them are equally efficient. However, if the neutralizing efficiency of the same amount of reagent under the same environmental conditions is compared, some subtle differences can be appreciated. A slower dissolution kinetics and lower final pHs can be observed if limestone and eggshells results are compared with the ones obtained for sea shells (clams and mussels, Fig. 14, Chapter 3). Also, sea shells are easier to find along Chile. For all these reasons, it was decided to select sea shells as the optimum $CaCO_3$ reagent to be used in the following experiments.

Table 3: Mean output water quality parameters from the 4 experiments performed to test different $CaCO_3$ reagents. The values recommended by the World health Organization (WHO, 2008) and the US environmental Protection Agency (USEPA, 2017) are also listed as references.

Reagent	pH	Fe (mg/L)	Al (mg/L)	Cu (mg/L)	Mn (mg/L)	Zn (mg/L)	SO_4^{2-} (mg/L)	Net acidity (mg/L of $CaCO_3$)*
Limestone	6.81 ± 0.08	0.125 ± 0.11	0.03 ± 0.01	0.015 ± 0.004	7.24 ± 0.43	0.99 ± 0.5	1179 ± 148	14.91 ± 1.36
Mussels Shells	7.34 ± 0.07	0.1 ± 0.14	0.03 ± 0.004	0.01 ± 0.002	6.63 ± 1.13	0.91 ± 0.66	1281 ± 336	13.89 ± 2.69
Clams Shells	7.34 ± 0.02	0.13 ± 0.16	0.03 ± 0.01	0.01 ± 0.002	5.86 ± 1.42	0.81 ± 0.33	1242 ± 293	12.38 ± 2.75
Egg Shells	7.11 ± 0.07	0.11 ± 0.11	0.02 ± 0.007	0.01 ± 0.004	6.99 ± 0.56	0.14 ± 0.04	1328 ± 231	13.33 ± 1.18
WHO-USEPA		0.3	0.1	2	0.05	5	250	

* Net Acidity=$50.045(3C_{Al}+2C_{Fe}+2C_{Mn}+2C_{Zn}+2C_{Cu}+10^{-pH})$-alk. C_X: molar concentrations. Modified from Rotting 2008a to consider Cu.
The values after the ± symbols correspond to the standard deviation of the mean values.

The detailed geochemistry controlling Fe and Al precipitation down the columns profiles (Fig. 11, Chapter 3) showed the same trends confirmed in many previous studies (i.e., an upper iron precipitation front controlled by schwertmannite followed by an aluminum precipitation front controlled by hydrobasaluminite). Therefore, it will not be discussed again on this work. However, the new AMD compositions used on the present experiments, more specifically the different ratios between dissolved elements and particularly the low Al/Cu ratio (Table 9, Chapter 3), induced a geochemical trend for Cu never observed before. This new Cu behavior was almost identical regardless the reactive material employed in the $CaCO_3$-DAS columns. Because of that and to avoid unnecessary redundant information, the following discussion will be focused just on the evolution of the geochemical profile of one selected column. To this end, the first column on experiment B.2 (Figure 4) was selected because the higher Al and Cu load used in this experiment could allow the better development of two differentiated precipitation fronts for these two elements.

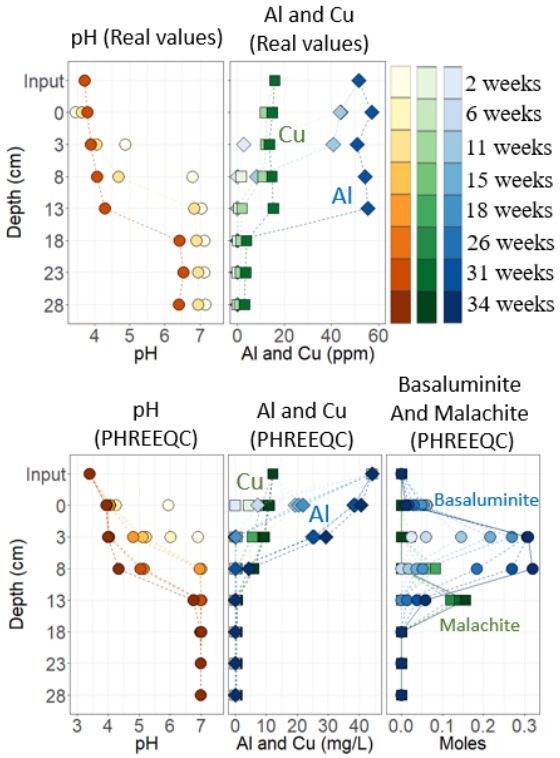

Figure 5: All the results correspond to the mussel shell-DAS column at experiment B.2. A) Spatial and temporal evolution of some representative operational parameters along the column, and B) Results obtained in the geochemical model performed with Phreeqc.

Previous studies have shown that copper precipitation typically mimics the precipitation profile showed by aluminum within the limestone-DAS columns [8,19]. This coupled behavior has been interpreted as Cu co-precipitation and/or sorption in hydrobasaluminite [19]. However, the profiles obtained in the present experiments cannot be exclusively explained by these processes, because sometimes, Cu total removal is obtained deeper in the column profile and after complete Al removal is achieved (Figure 5). Additionally, the results of a geochemical model perform to this mussels shells-DAS column anticipate the formation of a Cu precipitation front (made by malachite, $Cu_2CO_3(OH)_2$) right downward the hydrobasaluminite precipitation front (Figure 5).

To confirm or deny the precipitation of malachite within the $CaCO_3$-DAS columns (as well as the presence of other mineral phases), several mineralogical analyses were performed (Figure 6). Before that, a visual inspection of the DAS material during the solid sampling campaign revealed the expected "colored precipitation zone", showing the typical upper orange-reddish zone approximately from 0 to 5 cm depth (and made by precipitated schwertmannite) followed by a whitish zone roughly from 5 to 15 cm depth (made by hydrobasaluminite precipitates). A picture of the column just before the solid sampling campaign is shown in Figure 15 (Chapter 3). If some solid samples from the deeper section of the column are looked closely, small particles (shell and wood shaving pieces) coated with a green mineral can be observed (Figure 16, Chapter 3). These green crystals were separated from the main grain, and fizziness was observed when they were put in contact with a drop of 10% HCl (the expected reaction for malachite).

As in most previous studies, the XRD study of the remaining $CaCO_3$-DAS is characterized by an upper section (approximately down to 15-20 cm depth in this experiment) where the alkaline reagent (i.e., aragonite, $CaCO_3$) has been consumed and the only clearly discernible XRD signals (Fig. 6A) correspond to gypsum ($CaSO_4 \cdot 5H_2O$). Also, as usual, the diffractogram showed the typical high background and/or noise due to the presence of a big amount of very poorly crystalline phases like schwertmannite and hydrobasaluminite. However, for the first time, three very subtle peaks corresponding to malachite were identified on samples at 8-14 cm and 14-20 cm deep (Fig. 6A). The semiquantitative study performed to this sample is in accordance with the previous visual observations and the expected amount of malachite in both samples should be lower than 1% (Fig. 6B). Finally, the presence of malachite was also suggested by the data obtained using electron microscopy, where single particles made by Cu, C and O (detected by EDS) were observed (Fig. 6C).

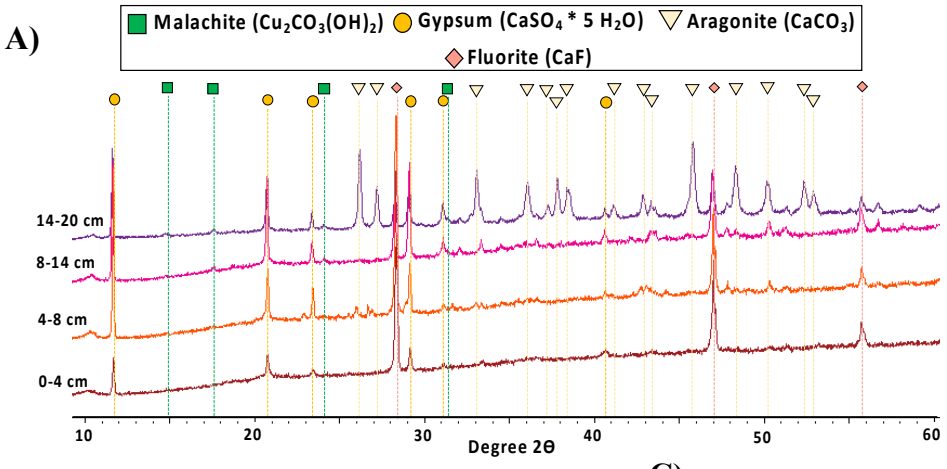

B)

Depth (cm)	Fluorite	Gypsum	Malachite	Aragonite	Amorphous
	(wt %)				
0-4	10.3	1.0			88.6
4-8	9.8	1.7			88.5
8-14	10.0	5.1	0.7		84.2
14-20	9.5	4.8	0.9	19.4	65.4

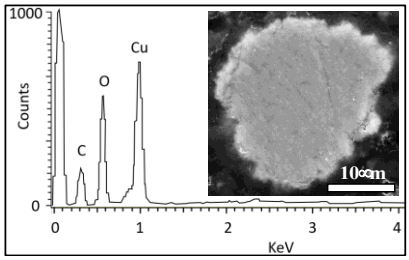

Figure 6: Mineralogical and chemical evidences of the presence of malachite within mussel shell-DAS column at experiment B.2. A) Stacked X-Ray diffractograms and mineral peaks assignment; B) Mineral semi-quantification using fluorite as internal standard; and C) EDS pattern and SEM electron backscattered image of a malachite single particle.

The most plausible reasons behind the precipitation, for the first time, of malachite in $CaCO_3$-DAS type columns are: 1) the significantly low Al/Cu ratio in the AMD used in the present experiments (Table 9), and 2) the higher alkalinity achieved in these experiments (around 300 mg/L as $CaCO_3$) comparing with other previous experiments (e.g., alkalinity in Monte Romero was around 100 mg/L as $CaCO_3$, [19]) where no malachite was detected.

2.3.2 Evaluation of the long-term removal of different loads of sulfate using $BaCO_3$-DAS

The only previous experience using witherite to remove SO_4^{2-} from AMD waters reported very promising results, showing an almost complete SO_4^{2-} water removal after the treatment (Torres et al., 2018). However, it is important to notice the low water inflow and operation time of the experiment (Table 1), as well as the intermediate sulfate concentration of the water entering the $BaCO_3$-DAS column (i.e., from the 5,000 mg/L of sulfate in the original AMD only 1,770 mg/L exits the $CaCO_3$-DAS column and enters the $BaCO_3$-DAS column). As a result, the $BaCO_3$-DAS column was submitted to a very modest sulfate load (0.7 g of SO_4^{2-} per day) on this experiment. To know the $BaCO_3$-DAS technology response when submitted to higher sulfate loads, the $BaCO_3$-DAS columns of the present study were designed to received 1.9 and 13.3 g/day of SO_4^{2-} (i.e., 2.7 and 19 times more sulfate than the experiment by Torres et al. 2018) [22].

To facilitate the explanation of the main findings during these multiple experiments, the results from experiment B.1 (sulfate load of 1.9 g/day) will be used to exemplify the general geochemical performance of the $BaCO_3$-DAS columns. According to equation (1) the main expected effects of witherite dissolution should be an increase on water pH and a decrease on sulfate concentration. In addition, the waters may also exhibit a local increase in the concentration of Ba (depending on the local final balance between witherite dissolution and barite precipitation) as well as some local decrease in Ca concentration as a result of $CaCO_3$ precipitation. Taking into account all these processes, it can be inferred that the $BaCO_3$-DAS column on experiment B.1 showed signs of witherite dissolution during the firsts 6 months of operation (Fig. 7A). During this period, the water outflowing the column always showed sulfate concentrations lower than 500 mg/L. However, if the geochemistry time series of the column are observed in detail, it can be observed how after 17 weeks of operation the sulfate concentration began to increase as water pH and exceeding dissolved Ba starts to decrease upward from the bottom of the column (Fig. 7A). This peculiar behavior cannot be explained by witherite exhaustion. As shown in the hydrochemical model performed (Fig. 7B), if the column would have progressively consumed the available witherite downward the column (as it did for the $CaCO_3$-DAS columns and during the early weeks of the $BaCO_3$-DAS experiments), it should have shown better sulfate removal and more steady water pHs (between 8 and 9) along the 38 weeks of the experiments.

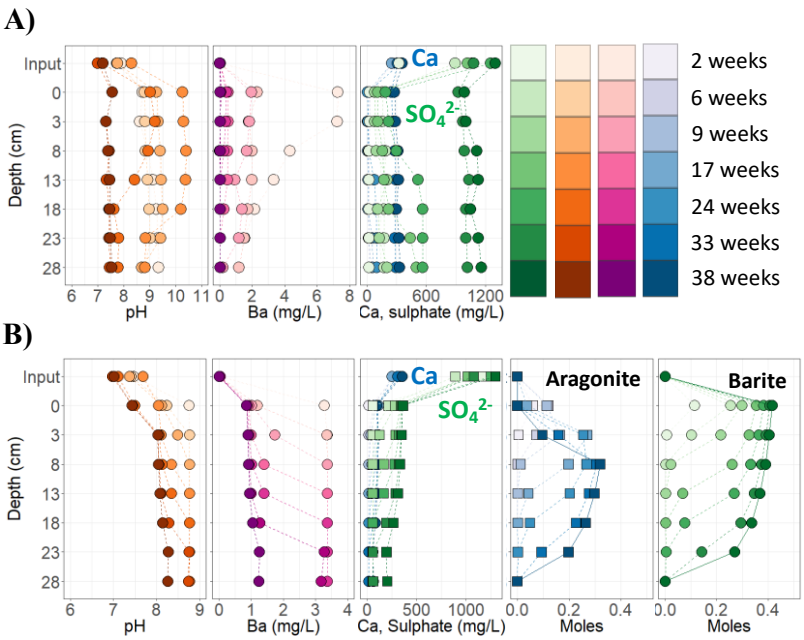

Figure 7: Raw (A) and modeled (B) hydrochemical depth profiles of the main operational parameters and elements within the $BaCO_3$-DAS column in experiment B.1. Notice that modeled precipitation profiles of barite ($BaSO_4$) and aragonite ($CaCO_3$) are shown in B), where positive values correspond to precipitated amount of mineral.

Also, it is important to notice that this evolution of the hydrochemical depth profiles is much faster in the $BaCO_3$-DAS column at experiment B.2 (Figure 17B, Chapter 3). Because of the higher sulfate load received by this column (13.3 g/day), the first signs of the reactive material exhaustion were observed after 11 weeks of operation and the remediation capacity of the column completely stopped after 18 weeks of operation. In addition, these figures show how both $BaCO_3$-DAS columns achieved an excellent Mn removal when witherite dissolution is actively occurring. Therefore, by using witherite the need of a MgO-DAS step to remove divalent metals (like Mn^{2+}) could be avoided.

To obtain a different perspective helping to explain the geochemical evolution of the column, several solid samples at different depths within the column were obtained and studied by XRD. During this solid sampling campaign, a visual inspection of the two $BaCO_3$-DAS columns allowed identifying two well differentiated vertical zones. The first zone (wall zone) corresponded to the reactive material close to the wall in contact with the inflowing water (notice that the design of the column induced that the inflowing water run down the wall of the column instead of directly dripping to the supernatant of the column, Figure 18). The second zone (core zone) corresponded to most of the column and it is characterized by a less cemented less compacted material (if compared with the samples from the wall zone). The semiquantitative mineralogical characterization of these samples are shown in Table 4. As can be observed, all the columns and sections are characterized by and almost complete or complete exhaustion of the original witherite as well as by the significant precipitation of $CaCO_3$ mineral phases (i.e., calcite and/or aragonite) and barite (Figures 12 and 13, Chapter 3). Both $BaCO_3$-DAS columns typically show higher amounts of $CaCO_3$ precipitates (calcite+aragonite) in the samples from the wall section (if compared with the sample from the core section). These results are in accordance with the visual observations during the sampling and could explain the higher cementation of the samples from the wall section. It is also important to notice that the $BaCO_3$-DAS column at experiment B.2 showed no signs of witherite in the wall section whereas some remaining witherite was detected in the samples from the core section.

Table 4: Mineralogical identification and semi-quantification of selected samples along the depth profile of the $BaCO_3$-DAS columns in experiments B.1 and B.2.

Experiment	Depth (cm)	Fluorite	Barite	Calcite	Aragonite	∑$CaCO_3$	Witherite	Amorphous
		(wt %)						
B.1	0-4	10.0	5.5		1.4	1.4	2.4	80.7
	4-8	9.5	1.2		4.0	4.0	1.1	84.3
	13-18	10.2	1.1		4.1	4.1		84.5
B.1_Wall	0-4	10.6	2.3		10.8	10.8	2.3	74.0
	4-8	10.8	1.8		8.7	8.7	3.8	74.9
	13-18	10.3	1.2		2.8	2.8	1.9	83.9
B.2	0-4	9.7	0.8	1.0	1.8	2.8	2.4	88.6
	4-8	10.6	9.1		2.2	2.2	1.1	88.5
	13-18	10.7	13.0		3.1	3.1	1.0	84.2
	23-30	9.6	2.2	2.1		2.1	2.7	65.4
B.2_Wall	0-4	10.9	5.2	0.7	0.5	1.2		84.2
	4-8	10.2	6.3	0.7	1.0	1.8		76.9
	13-18	9.6	1.5	2.0	4.2	6.1		72.2
	23-30	9.6	2.9	3.9		3.9		83.3

∑$CaCO_3$ = addition of calcite and aragonite concentrations (wt %). B.1 and B.2 correspond to samples obtained from the core of the column, whereas samples B.1_Wall and B.2_Wall were obtained close to the wall of the columns.

Another independent observation that could help explaining the geochemical behavior of the columns, is that during the columns operations they do not show any decrease or lose in their hydraulic conductivity, despite the important mineral precipitation within the columns. In addition, a different coloring of the reactive material within the columns was developed during the experiment. At the end of the experiment, it was possible to clearly differentiate the wall and core sections within the column (the wall section went darker whereas the core section maintained the original coloring of the reactive mixture).

Considering all these independent observations, the following plausible interpretation for the column geochemical behavior and evolution is offered: During the first months of operation (i.e., 24 and 11 weeks at experiment B.1 and B.2, respectively) the $BaCO_3$-DAS columns showed signs of witherite dissolution and accomplished sulfate output concentrations lower than 500 mg/L. However, these columns began to exhibit the effect of preferential flows and water mixing a few weeks earlier. As a result, from the sixth (B.1) and fourth (B.2) months to the last of the experiments the columns lost their remediation capacities, but they maintained their original hydraulic conductivity due to the generation of preferential flow paths.

Also, the experimental design allowed gaining a better understanding of the $BaCO_3$-DAS technology regarding its sulfate removal efficiency and lifetime. The information is graphically presented on Figure 8 but it is also shown *in extenso* in Table 10 (Chapter 3). Comparing the results in Figure 8, it can be observed how an increase in the sulfate load received by the columns implied a decrease in their lifetime (i.e., moment when the water outflowing the column reach a value higher than 500 mg/L, yellow circles on the figure). On the other hand, the $BaCO_3$-DAS column in experiment B.2 was able to achieve a higher accumulated removed sulfate load during its shorter operation time but it has to be considered that a double amount of witherite (i.e., 2kg instead of 1kg) was used on this experiment.

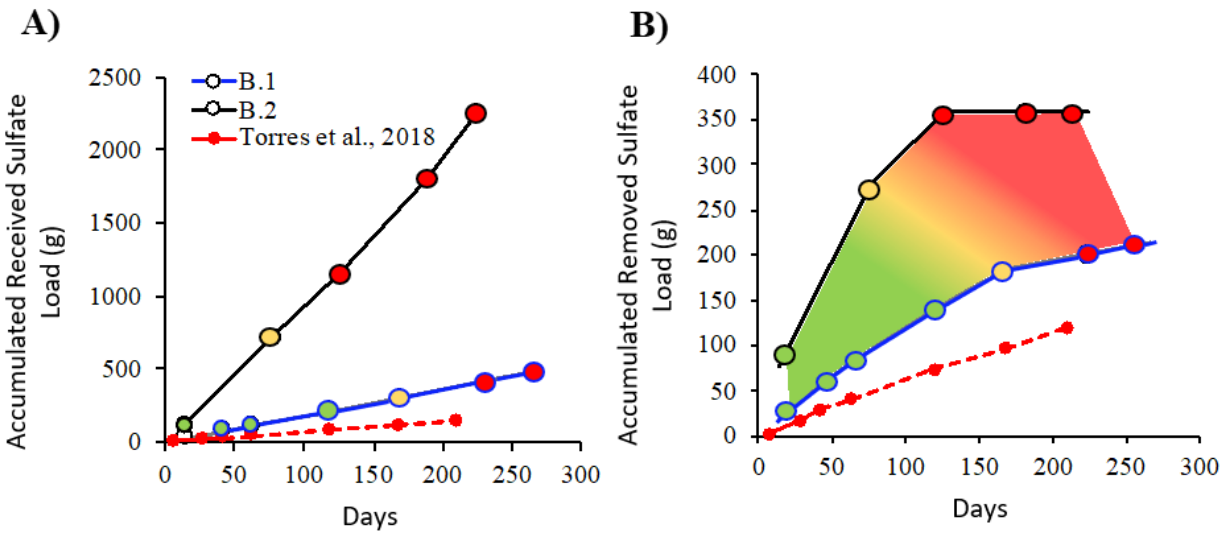

Figure 8: A) Accumulated received sulfate load and B) accumulated removed sulfate load in the two tested $BaCO_3$-DAS columns (i.e., B.1 and B.2) and the experiment by Torres et al., 2018. The circles colored in yellow and red mark the moments when the output sulfate concentrations reached values higher than 500 mg/L and 1000 mg/L, respectively. The dotted line in Torres et al., 2018 correspond to modeled data.

2.3.4 Implications, concluding remarks and future challenges

The present study has shown how other sources of $CaCO_3$ (i.e., mussel shells, clams shells and eggshells) might be as (or even more) efficient than limestone to remove Fe, Al and Cu from AMD polluted waters. These observations will facilitate the improvement of the DAS environmental footprint by reusing alternative by-product or residues (instead of mining raw materials) from local industries closer to the future full scale treatment locations.

It is also important to notice that, for the first time, malachite was confirmed as a mineral actively involved in the AMD remediation processes. This observation is of great importance for the optimum implementation of the DAS technology in AMDs with low to medium metal contents, because the mineralogical/geochemical reactions involved in the remediation process may be more diverse than previously thought. Therefore, it was confirmed that the implementation of a DAS-type technology is not straightforward, not only because the few operational parameters that have to be optimized and its working ranges defined (i.e., residence time, flowrate that can be treated or the reagent useful lifetime) but also because of new geochemical and mineralogical reaction that may be involved depending on the precise elemental composition and elemental ratio of the AMD to be treated.

Taking into consideration present and previous results, the $BaCO_3$-DAS reagent lifetime clearly depends on the sulfate load entering the system (i.e., higher sulfate loads = lower lifetime of the reagent material; Figure 8). Despite the observed generation of preferential flow paths within the $BaCO_3$-DAS columns, most of the available witherite was completely or almost completely consumed in the different sections of the columns (Table 4) achieving life times of up to 6 months. Therefore, although further investigations are necessary to avoid undesired preferential flow paths within the reactive mixture, this optimization is not expected to significantly extend the lifetime of the reactive mixture.

Regarding upscaling the present laboratory-scale experiments to a full scale field passive treatment systems, the accumulated removed sulfate load per volume of reactive mixture at the end of the system optimal performance was calculated (Table 10, Chapter 3). This parameter ranged between 0.035 and 0.053 g of SO_4^{2-}/cm^3 of $BaCO_3$-DAS. If the reactive mixture is assumed to present the same performance at field full-scale and AMDs with the same compositions of the present study are to be remediated, a 1,000 m^3 reactive pool (20m x 25m x 2,5m; length x width x depth) would be able to treat water inflows ranging from 3.3 to 11.8 L/s. This inflow rate are too low to remediate AMDs at active mine sites that typically exhibit flowrate of tens to hundreds of L/s. However, it perfectly fits the needs of abandoned and/or closed mine sites where the flow rates typically range between a few units to a few tens of L/s. Following this exercise and considering a cost of the commercial $BaCO_3$ reagent of 300 US$/t (https://www.alibaba.com/showroom/barium-carbonate-price.html), the cost of the needed $BaCO_3$ for the reactive pool treating 3.3 L/s of AMD would be around 50,000 US$. $BaCO_3$ current high price can be a serious obstacle for the economic feasibility of these type of passive treatment systems. However, several studies are setting the ground for the transformation of barite ($BaSO_4$) into witherite ($BaCO_3$) using a chemical engineering process based on the thermal reduction of $BaSO_4$ and $CaCO_3$ (combustion at 1,050 ºC in the presence of coal) transforming $BaSO_4$ into BaS. The bubbling of CO_2 in the resulting BaS aqueous slurry finally produce $BaCO_3$ and S [33,34]. Since the final residue of the $BaCO_3$-DAS treatment is rich in both barite and calcite, the regeneration of this material could be a plausible option improving the economic feasibility of the project under a circular economy perspective.

2.4. Acknowledgments

This study was funded by CORFO and Sacyr Chile through the project 16COTE-60128. It was also partially financed by the projects CONICYT/PIA Project AFB180004 and FONDECYT Initiation Project 11150002. The authors thank Mario Jara for their analytical assistance.

2.5. Bibliography

[1] Dold, B. (2014). Evolution of acid mine drainage formation in sulphidic mine tailings. *Minerals*, *4*(3), 621-641.

[2] Jacobs, J. A., Lehr, J. H., & Testa, S. M. (2014). *Acid mine drainage, rock drainage, and acid sulfate soils: causes, assessment, prediction, prevention, and remediation*. John Wiley & Sons.

[3] Skousen, J., Zipper, C. E., Rose, A., Ziemkiewicz, P. F., Nairn, R., McDonald, L. M., & Kleinmann, R. L. (2017). Review of passive systems for acid mine drainage treatment. *Mine Water and the Environment*, *36*(1), 133-153.

[4] Younger PL, Wolkersdorfer C (2004) Mining impacts on the fresh water environment: technical and managerial guidelines for catchment scale management. Mine Water Environ 23:s2–s80

[5] Akcil, A., & Koldas, S. (2006). Acid Mine Drainage (AMD): causes, treatment and case studies. *Journal of cleaner production*, *14*(12-13), 1139-1145.

[6] Younger PL, Banwart SA, Hedin RS (2002) Mine water: hydrology, pollution, remediation. Kluwer, Dordrecht, 442 pp.

[7] Ziemkiewicz, P.F., Skousen, J.G., Simmons, J., 2003. Long-term performance of passive acid mine drainage treatment systems. Mine Water and the Environment 22, 118-129.

[8] Ayora, C., Caraballo, M. A., Macias, F., Rötting, T. S., Carrera, J., & Nieto, J. M. (2013). Acid mine drainage in the Iberian Pyrite Belt: 2. Lessons learned from recent passive remediation experiences. *Environmental Science and Pollution Research*, *20*(11), 7837-7853.

[9] Johnson, D. B., & Hallberg, K. B. (2005). Acid mine drainage remediation options: a review. *Science of the total environment*, *338*(1-2), 3-14.

[10] Kefeni, K. K., Msagati, T. A., & Mamba, B. B. (2017). Acid mine drainage: prevention, treatment options, and resource recovery: a review. *Journal of Cleaner Production*, *151*, 475-493.

[11] Gazea, B., Adam, K., & Kontopoulos, A. (1996). A review of passive systems for the treatment of acid mine drainage. *Minerals engineering*, *9*(1), 23-42.

[12] Skousen, J., & Ziemkiewicz, P. (2005). Performance of 116 passive treatment systems for acid mine drainage. *Proceedings, American Society of Mining and Reclamation, Breckenridge, CO*, 1100-1133.

[13] Sheoran, A. S., & Sheoran, V. (2006). Heavy metal removal mechanism of acid mine drainage in wetlands: a critical review. *Minerals engineering*, *19*(2), 105-116.

[14] Simón, M., Martín, F., García, I., Bouza, P., Dorronsoro, C., & Aguilar, J. (2005). Interaction of limestone grains and acidic solutions from the oxidation of pyrite tailings. *Environmental pollution*, *135*(1), 65-72.

[15] Rose, A.W., D. Bisko, A. Daniel, M.A. Bower, and S. Heckman. 2004. An "autopsy" of the failed Tangaskootack #1 vertical fl ow pond, Clinton Co., Pennsylvania. p. 1580–1594. In R.I. Barnhisel (ed.) Joint Conference of the 21st Annual Meetings of the American Society of Mining and Reclamation and 25th West Virginia Surface Mine Drainage Task Force Symposium, Morgantown, WV. ASMR, Lexington, KY.

[16] Rötting, T. S., Thomas, R. C., Ayora, C., & Carrera, J. (2006a). Challenges of passive treatment of metal mine drainage in the Iberian Pyrite Belt (Southern Spain): preliminary studies. In *Proc. of the Seventh Int. Conf. on Acid Rock Drainage, St. Louis, MO* (pp. 1753-1767).

[17] Rötting, T. S., Cama, J., Ayora, C., Cortina, J. L., & De Pablo, J. (2006b). Use of caustic magnesia to remove cadmium, nickel, and cobalt from water in passive treatment systems: column experiments. *Environmental science & technology*, *40*(20), 6438-6443.

[18] Rötting TS, Thomas RC, Ayora C, Carrera J (2008a) Passive treatment of acid mine drainage with high metal concentrations using dispersed alkaline substrate. J Environ Qual 37:1741–1751

[19] Caraballo, M. A., Rötting, T. S., Nieto, J. M., & Ayora, C. (2009). Sequential extraction and DXRD applicability to poorly crystalline Fe-and Al-phase characterization from an acid mine water passive remediation system. *American Mineralogist*, *94*(7), 1029-1038.

[20] Caraballo, M. A., Macías, F., Nieto, J. M., Castillo, J., Quispe, D., & Ayora, C. (2011). Hydrochemical performance and mineralogical evolution of a dispersed alkaline substrate (DAS) remediating the highly polluted acid mine drainage in the full-scale passive treatment of Mina Esperanza (SW Spain). *American Mineralogist*, *96*(8-9), 1270-1277.

[21] Macías, F., Caraballo, M. A., Rötting, T. S., Pérez-López, R., Nieto, J. M., & Ayora, C. (2012). From highly polluted Zn-rich acid mine drainage to non-metallic waters: Implementation of a multi-step alkaline passive treatment system to remediate metal pollution. *Science of the total environment*, *433*, 323-330.

[22] Torres, E., Lozano, A., Macías, F., Gomez-Arias, A., Castillo, J., & Ayora, C. (2018). Passive elimination of sulfate and metals from acid mine drainage using combined limestone and barium carbonate systems. *Journal of Cleaner Production*, *182*, 114-123.

[23] Rötting, T. S., Caraballo, M. A., Serrano, J. A., Ayora, C., & Carrera, J. (2008b). Field application of calcite Dispersed Alkaline Substrate (calcite-DAS) for passive treatment of acid mine drainage with high Al and metal concentrations. *Applied Geochemistry*, *23*(6), 1660-1674.

[24] Caraballo, M. A., Rötting, T. S., & Silva, V. (2010). Implementation of an MgO-based metal removal step in the passive treatment system of Shilbottle, UK: Column experiments. *Journal of hazardous materials*, *181*(1), 923-930.

[25] Ayora, C., Macías, F., Torres, E., Lozano, A., Carrero, S., Nieto, J. M., ... & Castillo-Michel, H. (2016). Recovery of rare earth elements and yttrium from passive-remediation systems of acid mine drainage. *Environmental science & technology*, *50*(15), 8255-8262.

[26] Valenzuela, M (2019). MsC mining thesis "*Monitoreo ambiental y análisis espacio temporal de la calidad hídrica de la cuenca del Mapocho".* Graduated. Universidad de Chile, Santiago.

[27] Martínez, N. M., Basallote, M. D., Meyer, A., Cánovas, C. R., Macías, F., & Schneider, P. (2019). Life cycle assessment of a passive remediation system for acid mine drainage: Towards more sustainable mining activity. *Journal of Cleaner Production*, *211*, 1100-1111.

[28] Camus, F., & Dilles, J. H. (2001). A special issue devoted to porphyry copper deposits of northern Chile. *Economic Geology*, *96*(2), 233-237.

[29] Barra, F., Reich, M., Selby, D., Rojas, P., Simon, A., Salazar, E., & Palma, G. (2017). Unraveling the origin of the Andean IOCG clan: A Re-Os isotope approach. *Ore Geology Reviews*, *81*, 62-78.

[30] Parkhurst, D. L., & Appelo, C. A. J. (2013). *Description of input and examples for PHREEQC version 3: a computer program for speciation, batch-reaction, one-dimensional transport, and inverse geochemical calculations* (No. 6-A43). US Geological Survey.

[31] WHO, World Health Organization, 2008. Guidelines for Drinking-water Quality. Fourth Edition. Retrieved from. http://www.who.int/water_sanitation_health/ dwq/fulltext.pdf.

[32] USEPA. U.S. Environmental Protection Agency, 2017. National Drinking Water Regulations. Retrieved from. https://www.epa.gov/dwstandardsregulations.

[33] Masukume, M., Maree, J.P., Ruto, S., Joubert, H., 2013. Processing of barium sulphide to barium carbonate and sulphur. Chem. Eng. Proc. Technol. 4, 157. https://doi.org/10.4172/2157-7048.1000157.

[34] Mulopo, J., 2015. Continuous pilot scale assessment of the alkaline barium calcium desalination process for acid mine drainage treatment. J. Environ. Chem. Eng. 3, 1298-1302

Capítulo 3

Material suplementario

3.1 Columns and decantation ponds setups

Polymethyl methacrylate cylinders (15cm inner diameter, 50cm in height) were used as the basis for the experiment. Each cylinder/column has a plastic three way valve every 5cm on the outer part, so each column has 8 valves used for measurements. Inside the column, from bottom to top, there are 3cm of coarse-grained quartz and 30cm of substrate, that is to say, the mixture of wood shavings (the inert material) and the reactive material. The rest of the column consist of the supernatant and free space. All columns and decantation vessels were open to the atmosphere.

The input synthetic AMD was pumped using peristaltic pumps (Masterflex L/S 07557-14) and from there the water flowed by gravity. As seen in Figure 4, the water passes from the DAS carbonated columns towards a decantation vessel and then to the witherite columns.

Figure 9: DAS column before starting the experiment (mixture of wood shavings and clam shells). On the left side, 9 sampling ports can be observed (blue three way valves). The distance between sampling ports was 5 cm.

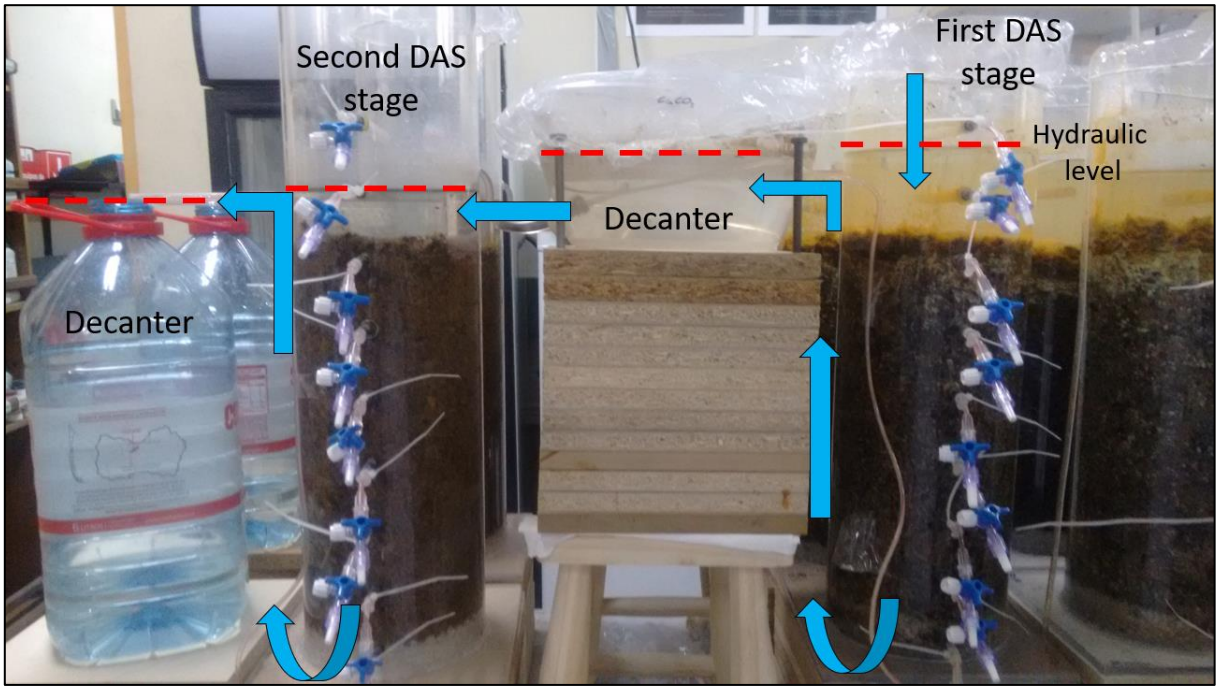

Figure 10: General picture of the experimental set up. The red line represents the hydraulic level, while the blue arrows represent the path of water from the input (upper right) to the output (left side).

Table 5: Input synthetic AMD (x in Fig. 4)

Element	**Concentration (mg/L)**
Fe	10.11
Al	25.8
Ca	212
Mn	7.1
Mg	58.4
Zn	2.6
Cu	7.9
Ni	0.01
Co	0.02
As	0.16
SO_4^{2-}	1234
pH	3.7
Conductivity (mS/cm)	2.2

ELEMENT	DETECTION LIMIT
Ag	0.05 ppb
Al	1 ppb
As	0.5 ppb
Au	0.05 ppb
B	5 ppb
Ba	0.05 ppb
Be	0.05 ppb
Bi	0.05 ppb
Br	5 ppb
Ca	0.05 ppm
Cd	0.05 ppb
Ce	0.01 ppb
Cl	1 ppm
Co	0.02 ppb
Cr	0.5 ppb
Cs	0.01 ppb
Cu	0.1 ppb
Dy	0.01 ppb
Er	0.01 ppb
Eu	0.01 ppb
Fe	10 ppb
Ga	0.05 ppb
Gd	0.01 ppb
Ge	0.05 ppb
Hf	0.02 ppb
Hg	0.1 ppb
Ho	0.01 ppb
In	0.01 ppb
K	0.05 ppm
La	0.01 ppb
Li	0.1 ppb
Lu	0.01 ppb
Mg	0.05 ppm
Mn	0.05 ppb
Mo	0.1 ppb

ELEMENT	DETECTION LIMIT
Na	0.05 ppm
Nb	0.01 ppb
Nd	0.01 ppb
Ni	0.2 ppb
P	10 ppb
Pb	0.1 ppb
Pd	0.2 ppb
Pr	0.01 ppb
Pt	0.01 ppb
Rb	0.01 ppb
Re	0.01 ppb
Rh	0.01 ppb
Ru	0.05 ppb
S	1 ppm
Sb	0.05 ppb
Sc	1 ppb
Se	0.5 ppb
Si	40 ppb
Sm	0.02 ppb
Sn	0.05 ppb
Sr	0.01 ppb
Ta	0.02 ppb
Tb	0.01 ppb
Te	0.05 ppb
Th	0.05 ppb
Ti	10 ppb
Tl	0.01 ppb
Tm	0.01 ppb
U	0.02 ppb
V	0.2 ppb
W	0.02 ppb
Y	0.01 ppb
Yb	0.01 ppb
Zn	0.5 ppb
Zr	0.02 ppb

Figure 11: Detection limits reported by ActLabs for their analytical package ICP-MS and ICP-OES S0200 for natural waters.

3.2 X-Ray Diffraction mineral phases identifications and semiquantitative analyses

To obtain the best possible mineral quantification, it was decided to add an internal standard to each sample to be analyzed by XRD. All the solid samples were doped with a 10 wt% of fluorite. By the addition of this standard, it was possible to correct minor drifts on the diffractograms improving the peaks assignments. Despite the use of this internal standard the results were interpreted as semiquantitatives because of two main problems affecting the calculations:

1) The used fluorite standard did not perfectly match the information for fluorite available on the selected database (PDF2.dat). As a result, peaks intensity distributions slightly change, affecting the quantification calculations (fluorite concentrations higher than 10 wt% were always observed).

2) All the peaks corresponding to barite systematically showed a slight displacement to lower 2Θ values. This effect has to be related with the mineral itself because any shift from the instrument and/or the analyst was corrected by the use of the internal standard. A plausible explanation to this shifting could be a minor substitution of Ba by Ca in the structure of barite. Disregarding the exact cause of this imperfect fitting between the diffractogram peaks and the information in the database, barite quantification showed lower values than it could be expected.

To obtain the final semiquantitative results shown in the present study (Figure 6 and Table 4 on the main manuscript), the results were normalized to adjust fluorite wt% to the real values added to each sample.

Also, due to this analyses difficulties, the final proportion of the sample considered as amorphous typically showed very high values for this type of samples, where the amorphous component of the signal could mainly be attributed to the presence of wood shaving.

As a consequence of all these adjustments, whereas mineral phases identification were very solid, it was decided to consider the results as semiquantitatives and their interpretations and discussion were made with great caution.

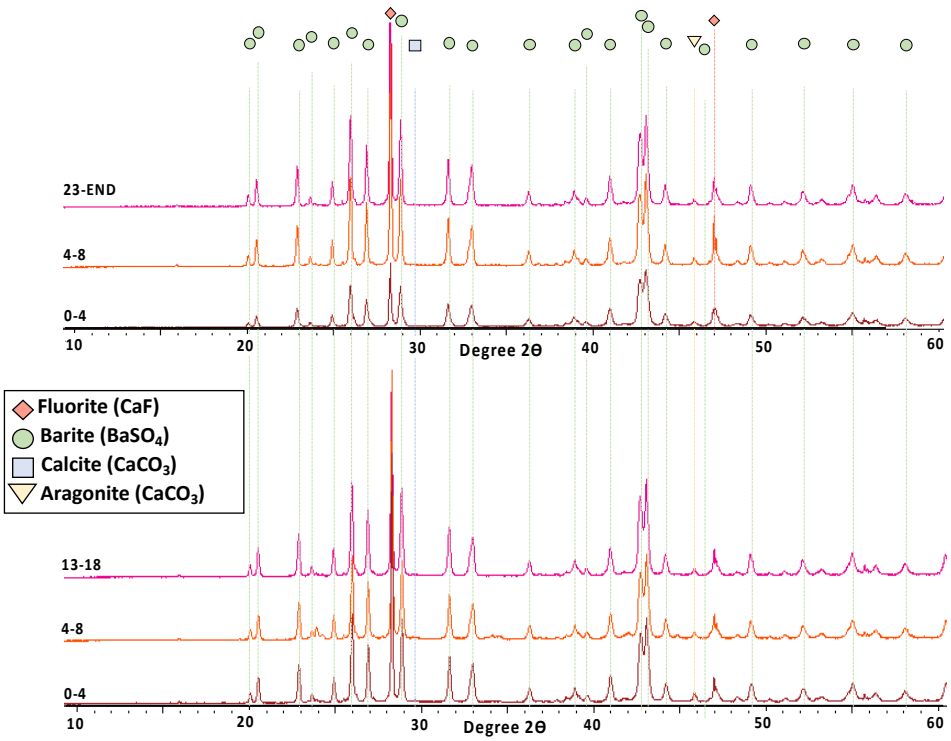

Figure 12: X-Ray diffractograms for samples B.1 (core zone, upper graphic) and B.1_Wall (wall zone, lower graphic).

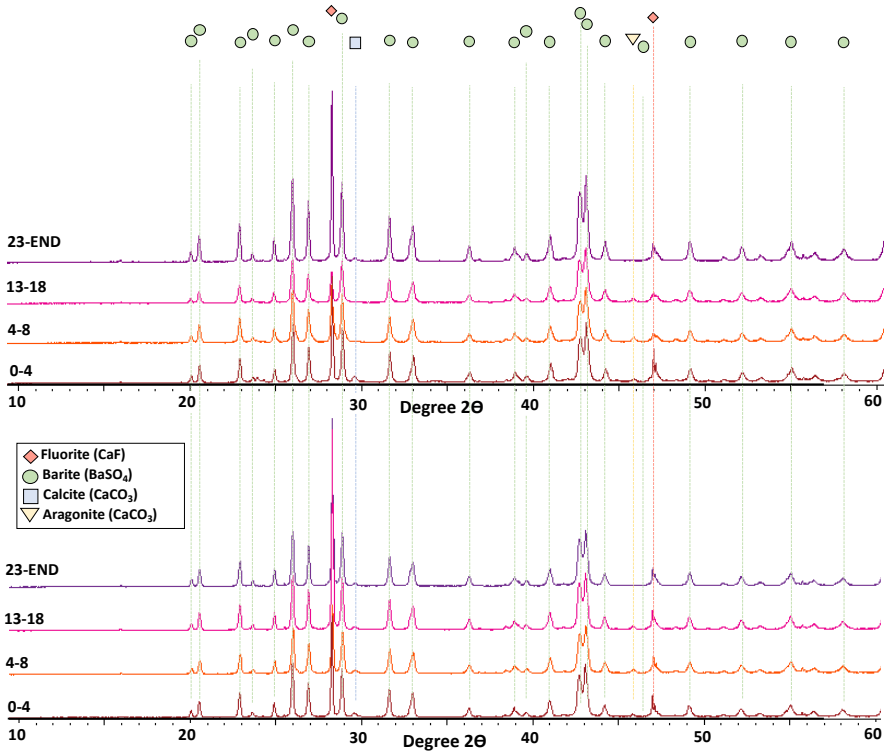

Figure 13: X-Ray diffractograms for samples B.2 (core zone, upper graphic) and B.2_Wall (wall zone, lower graphic).

3.3 Geochemical model

Leaching behavior interpretations and modelling require simultaneous consideration of several transport and chemical equations with different complexity levels. In most cases, the chemical reactions involved are complex and abundant, and high-performance numerical tools coupled with huge thermodynamic data bases are needed. Over the last decades, several modelling tools for these complex aqueous chemistry problems have been developed, and many geochemical software are available nowadays (e.g. MINTEQA2, EQ3/6, WATEQ4F, Geochemist's workbench, CHESS, PHREEQC, among many others).

The geochemical software PHREEQC allows coupling the full geochemical model with certain transport phenomena, allowing to simulate percolation (with a constant flow) or diffusion in some simple systems while keeping the numerical performances. It is also compatible with several data bases and has the extra advantage of being open source. For these reasons, PHREEQC was selected in the present research.

3.3.1 Dynamic leaching tests and scenarios

This leaching experiment involves the construction of two cells with a granular monolithic sample with continuous renewal of the leaching solution. The total time of the experiment was between 34-38 weeks. The main characteristics of the leaching solutions and the granular materials considered in the geochemical model are shown in table 6.

Table 6: Main characteristics of the leaching solutions and the granular materials considered in the geochemical model.

	Leaching solutions		Granular materials			
	Type	Flux (L/day)	Type	Reactive material amount (g)	Porosity	Specific surface (cm^2/L)
Case #1	Acidic and high metal concentration	5.4	CaCO3-DAS	1,115	0.56	16,700
Case #2	Neutral and high sulfate concentration	1.5	BaCO3-DAS	1,000	0.8	6,500

A 1D reactive transport model consisting on several concatenated cells was created. This 1D model was submitted to a changing input solution, and the following equilibrium reactions are allowed for a time Δt:

Reaction allowed in Case#1

Aragonite: $CaCO_3 = CO_3^{-2} + Ca^{+2}$

Schwertmannite: $Fe_8O_8(OH)_{4.5}(SO4)_{1.75} + 20.5H^+ = 8Fe^{+3} + 12.5H_2O + 1.75SO_4^{-2}$

Basaluminite: $Al_4(OH)_{10}SO_4 + 10H^+ = 4Al^{+3} + 10H_2O + SO_4^{-2}$

Malachite: $Cu_2CO_3(OH)_2 + 3H^+ = HCO_3^- + 2Cu^{+2} + 2H_2O$

Reactions allowed in Case#2

Witherite: $BaCO_3 = Ba^{+2} + CO_3^{-2}$

Barite: $BaSO_4 = Ba^{+2} + SO_4^{-2}$

Gypsum: $CaSO_4{:}2H_2O = Ca^{+2} + SO_4^{-2} + 2H_2O$

In each cell, when the leaching solution reaches the reactive material, the dissolution/precipitation processes begin at the solid/porewater interface together with chemical reactions (acid/base, complexation, redox) in the aqueous phase. The surface of the material in each cell is in contact with the leaching solution, which usually represents an aggressive solution because its composition is generally very different from that of the equilibrium situation.

The chemical speciation at equilibrium is defined by a set of equations representing the mass balance law (equilibrium constants) for each chemical element and the electrical charge balance. The set of equilibrium equations is resolved by the Newton–Raphson algorithm and the result is the concentration of each chemical species in each phase including the pH and the pe.

The integration of kinetic equations over time is executed by a Runge-Kutta algorithm. The partial differential equations describing the transport processes are resolved by an explicit finite difference algorithm. Therefore, the behaviour of the system was controlled by the slower dissolution of $BaCO_3$. The amount (m) of barium carbonate dissolved (mol/m^3·s) was calculated as:

$$m = A * r * (1 - \Omega)$$

Where A is the reactive surface area (m^2/m^3 column), Ω is the saturation index of the solution, and r is the dissolution rate (mol/m^2/s) obtained for witherite and calcite by Plummer et al. (1978) and approximated as:

$$Witherite: \; r = 10^{-1.32}a_{H^+} + 10^{-4.59}a_{CO_2} + 10^{-6.94}a_{H_2O}$$
$$Calcite: r = 10^{-1.32}a_{H^+} + 10^{-4.59}a_{CO_2} + 10^{-6.94}a_{H_2O}$$

In order to calculate both equilibrium and dynamic processes a split-operator scheme is used. At each time step (the time grid is calculated following numerical stability and dispersion criteria) the kinetic and equilibrium reactions are calculated after the advection and dispersion step.

Finally, the geochemical aspects of equilibrium and kinetic phases considered from the experimental observations are presented below (Table 7). Similarly, the hydraulic characteristics of the transport model are obtained from the experimental conditions and are presented in Table 8.

Table 7: Kinetics and equilibrium phases imposed.

	Case 1	Case 2
Kinetics	Carbonate	Witherite
	Basaluminite	Aragonite
Equilibrium Phases	Gypsum	Barite
	Malachite	Gypsum
	Schwertmannite	Haussmannite

Table 8: Dynamic characteristics of cells for transport conditions.

	Case 1	Case 2
Total Leachate Volume (L)	3.6	4.5
Darcy flow speed (cm/day)	51	10.4
Time between ports (h)	1.1	8.2
N° of transport cells	7	6
Diffusion coefficient (m^2/s)	3e-10	3e-10
Flow direction	Forward	Forward

3.4 Assessment of $CaCO_3$ rich residues from agri-food industries treating an Andean AMD with intermediate metals and sulfate concentrations

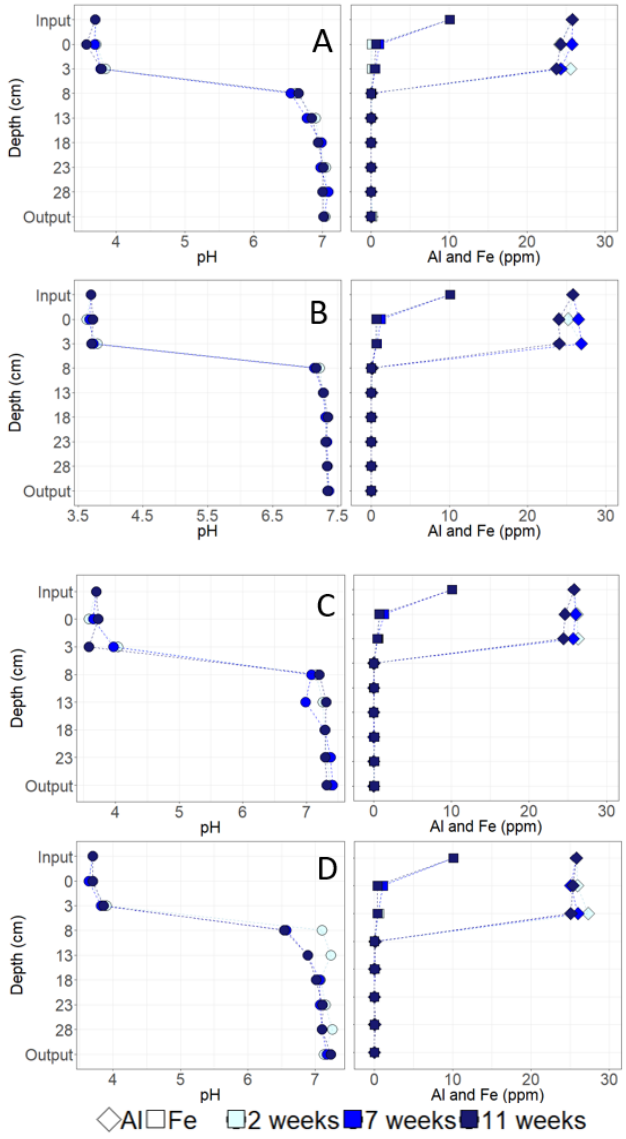

Figure 14: Results for pH, Fe and Al for each reactive material used. A: Calcite column, B: Clam shell column, C: Mussel shell column, D: Eggshell column

Table 9: Comparison of net acidity, Al, Cu and Al/Cu ratios between different DAS experiences.

Source	Study site	Al (mg/L)	Cu (mg/L)	Al/Cu ratio	Net acidity (as $CaCO_3$)*
Rotting 2008	Monte Romero	75	1.5	50	1400-1600
Caraballo 2009	Monte Romero	117	10	11.7	2500
Caraballo 2011	Mina Esperanza	128-167	12-24	10.6-6.9	2300
Macias 2011	Monte Romero	100	5	20	1800
Macias 2012	Monte Romero	70-91	2.1-3.4	33.3-26.7	1404-1609
Ayora 2016	Monte Romero	128	7	18.28	1800
Torres 2018	Almagrera	532	0.096	5541	5000
Present Study	Column setup	25.8-51.6	7.9-15.8	**3.2**	202-404

* Net Acidity=$50.045(3C_{Al}+2C_{Fe}+2C_{Mn}+2C_{Zn}+2C_{Cu}+10^{-pH})$-alk. C_X: molar concentrations. Modified

Figure 15: Mussel shell-DAS column at experiment B.2 right before the solid sampling campaigns. The iron (orange) and aluminum (white) precipitation fronts can be observed. Notice that some schwertmannite (orange precipitates) reached deeper in the column using some preferential paths created on the walls but the two precipitation fronts were better defined in the column core (away from the walls).

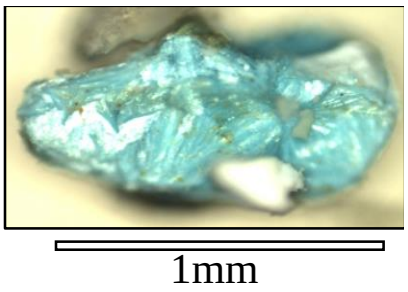

Figure 16: Picture of a grain covered by green crystals obtained with a magnification binocular microscope.

3.5 Evaluation of the long-term removal of different loads of sulfate using $BaCO_3$-DAS

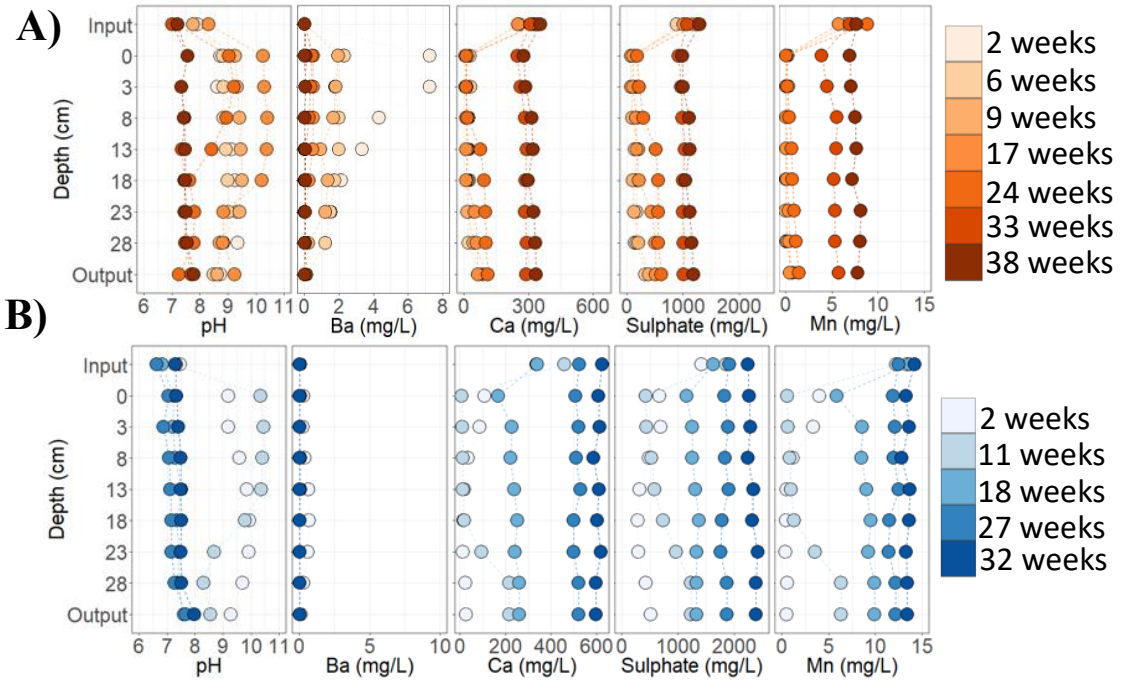

Figure 17: Time evolution of the chemical depth profiles for the $BaCO_3$-DAS columns in experiments: A) B.1 = 1.9 kg/day of sulfate load and B) B.2 = 13.3 kg/day of sulfate load.

Figure 18: Witherite Column at the end of the experiment.

Table 10: Accumulated sulfate load received and retained by the $BaCO_3$-DAS columns.

Experiment	Operation time (days)	Recieved SO_4^{2-} load (g)	Remove SO_4^{2-} load (g)	Removed SO_4^{2-} load (g/cm^3)
B.1	14	25	19	
	42	75	57	
	63	113	82	
	119	214	140	
	168	302	**184**	0.035
	231	415	203	
	266	478	214	
B.2	14	113	76	
	77	755	**280**	0.053
	126	1149	360	
	189	1795	360	
	224	2249	360	
Torres et al., 2018	7	3	3	
	28	18	18	
	42	30	30	
	63	44	40	
	119	83	73	
	168	116	97	
	210	144	120	0.083

Numbers in red correspond to modeled data

Capítulo 4

4.1 Conclusiones

La implementación realizada a escala de laboratorio del sistema de tratamiento pasivo para drenajes ácidos mineros DAS hace aun mas robusta esta tecnología. Estos avances permiten que una futura implementación del sistema en Chile sea viable, además de entregar información valiosa para cualquier estudio y eventual implementación del DAS en otras partes del mundo. A continuación, se presentan estos avances y algunas recomendaciones:

- Existen alternativas al uso de materiales reactivos como agentes para aumentar el pH del agua y así generar la retención de metales en el sustrato. Estos materiales incluyen cáscara de huevo y 2 tipos de conchillas, como materiales carbonatadas como alternativa al uso de calcita en la primera etapa de tratamiento DAS, la cual tiene como objetivo aumentar el pH a valores neutros y generar la retención de metales trivalentes. La viabilidad real del uso de estos materiales dependerá de las condiciones del lugar de eventual implementación, en donde factores económicos son los que serán de vital relevancia para la toma de decisión. El suministro del material a utilizar (una cantera para calcita o el mar/actividad pesquera para conchillas marinas, por ejemplo), las distancias y el enfoque medioambiental que se desee implementar determinaran el uso de uno u otro material. Independientemente de aquello, se logro probar que existe una alternativa real para utilizar otro tipo de materiales en la implementación del DAS a los ya conocidos, por lo que el uso de los materiales probados en este estudio, así como también otros que puedan ser viables en otras partes del mundo, se recomienda y visibiliza mucho más de lo que se venía haciendo en estudios DAS anteriores.

-Además, el estudio de estos materiales en la etapa $CaCO_3$-DAS mostro la presencia de un nuevo mineral que no se había detectado anteriormente en este tipo de sistemas: Malaquita. Esto muestra que es relevante el estudio continuo desde un punto de vista hidroquimico (y eventualmente mineralógico, claramente) del agua que ingresa al sistema, así como también las razones entre elementos de interés (en este caso, la relación entre Al y Cu). Diferentes razones entre elementos pueden generar la precipitación de nuevos minerales desconocidos en este tipo de sistemas y por lo tanto un continuo monitoreo y entendimiento del agua a tratar es crucial para no solo entender bien el sistema, sino también para evitar eventuales problemas que puedan ocurrir.

-De este último punto se desprende la necesidad de no asumir que por tener aguas que a primera vista pueden parecer similares, el sistema funcionara de la forma en que se espera. Este tipo de estudios muestran claramente que no por trabajar con una acidez neta menor a los estudios anteriores significa que no habrá sorpresas en los minerales encontrados. En un caso hipotético, una implementación del DAS en otra parte del mundo podría generar algún mineral de arsénico, lo cual puede ser relevante y lo cual implicaría un cuidado mucho mas elevado en el manejo del sistema y sus residuos.

-Respecto a la segunda etapa de tratamiento $BaCO_3$-DAS, el uso de witherita es efectivo en la retención de sulfato por un periodo de hasta 6 meses, en contraste al solo 1 mes y medio de buen funcionamiento probado hasta ahora en estudios anteriores. Se debe tener presente que estos tiempos estarán directamente relacionados a la carga de sulfato recibida por el sistema, por lo que la vida útil del mismo dependerá directamente de ello. Cambios en el AMD de entrada podrían afectar enormemente el tiempo de funcionamiento del sistema y por lo tanto un buen monitoreo debe ser un foco importante en la eventual implementación del sistema.

-Se debe tener en cuenta la generación de flujos preferenciales en la segunda etapa de tratamiento $BaCO_3$-DAS, en donde su solución variara dependiendo de las características del diseño del eventual sistema de tratamiento a escala real. Se debe tener en cuenta que la generación de estos flujos preferenciales puede ayudar a que el sistema funcione de forma óptima, lo cual eventualmente podría alargar la vida útil del sistema en muy menor medida. Considerando esta situación, se debe evaluar si realmente es económicamente viable el encontrar una solución al problema de flujos preferenciales.

-El costo económico de la witherita resulta el principal problema para su implementación, en donde será clave un buen estudio de mercado y un eventual estudio para reutilizar la barita de desecho del sistema para volver a obtener el material reactivo. Esto ultimo puede brindarle una vida cíclica al sistema DAS, con la desventaja de un alto consumo energético para realizar esta transformación mineral. Es por esto que se recomienda un estudio más acabado al respecto para poder determinar si es recomendable sacrificar el concepto de bajo consumo energético del sistema para poder tratar los propios desechos, en comparación al costo económico y huella de carbono relacionado al importar el material reactivo desde otras partes del mundo.

-Es importante destacar que el desafío futuro que plantea esta investigación es la eventual implementación de este sistema a escala piloto, es decir, enfrentar los problemas de escalamiento que eventualmente podrían cambiar las condiciones del sistema, como lo pueden ser procesos evaporíticos, variaciones del clima, materiales a utilizar en la construcción de los tanques, etc.

4.2 Bibliografía

Aubé, B., Lamares, M., & Lone Sang, S. (2018). A Pilot Optimisation of Sulphate Precipitation in the High-Density Sludge Process. *11th ICARD| IMWA| MWD*.

Ayora, C., Caraballo, M. A., Macias, F., Rötting, T. S., Carrera, J., & Nieto, J. M. (2013). Acid mine drainage in the Iberian Pyrite Belt: 2. Lessons learned from recent passive remediation experiences. *Environmental Science and Pollution Research*, *20*(11), 7837-7853.

Caraballo, M. A., Macías, F., Nieto, J. M., Castillo, J., Quispe, D., & Ayora, C. (2011). Hydrochemical performance and mineralogical evolution of a dispersed alkaline substrate (DAS) remediating the highly polluted acid mine drainage in the full-scale passive treatment of Mina Esperanza (SW Spain). *American Mineralogist*, *96*(8-9), 1270-1277.

Chien L et al. (1968) Infantile gastroenteritis due to water with high sulfate content. Canadian Medical Association Journal, 99:102–104.

Dold, B. (2003). Aguas Ácidas: formación, predicción, control y prevención. *Revista Minería*, *310*, 29-37.

Esteban E et al. (1997) Evaluation of infant diarrhoea associated with elevated levels of sulfate in drinking water: a case control investigation in South Dakota. International Journal of Occupational Medicine and Environmental Health, 3(3):171–176.

Fingl E (1980) Laxatives and cathartics. In: Gilman AG et al., eds. Pharmacological basis of therapeutics. New York, NY, MacMillan Publishing.

Gutierrez, F, Pincetti, G. Payacán, I. Tristram, E. Vela, I. (2015). Composición natural de las aguas en la cuenca alta del santuario de la naturaleza Yerba Loca, Santiago. *XIV Congreso geológico chileno.*

Larson, T.E. Corrosion phenomena -- causes and cures. In: Water quality and treatment. A handbook of public water supplies. 3rd edition. McGraw-Hill Publishing Co., New York, NY (1971).

Leistel, J. M., Marcoux, E., Thiéblemont, D., Quesada, C., Sánchez, A., Almodóvar, G. R., ... & Sáez, R. (1997). The volcanic-hosted massive sulphide deposits of the Iberian Pyrite Belt Review and preface to the Thematic Issue. *Mineralium Deposita*, *33*(1), 2-30.

Liu, Z., Li, L., Li, Z., & Tian, X. (2017). Removal of sulfate and heavy metals by sulfate-reducing bacteria in an expanded granular sludge bed reactor. Environmental Technology, 39(14), 1814–1822. doi:10.1080/09593330.2017.1340347

National Academy of Sciences. Drinking water and health. National Research Council, Washington, DC (1977).

Smith, B. L. (1980). Effect of high concentrations of zinc sulphate in the drinking water of grazing yearling dairy cattle. *New Zealand journal of agricultural research*, *23*(2), 175-178.

Taylor, J., Pape, S., & Murphy, N. (2005, August). A summary of passive and active treatment technologies for acid and metalliferous drainage (AMD). In *5th Australian workshop on Acid Mine Drainage, Fremantle, Australia*.

Torres, E., Lozano, A., Macías, F., Gomez-Arias, A., Castillo, J., & Ayora, C. (2018). Passive elimination of sulfate and metals from acid mine drainage using combined limestone and barium carbonate systems. *Journal of Cleaner Production*, *182*, 114-123.

US EPA (1999a) Health effects from exposure to high levels of sulfate in drinking water study. Washington, DC, US Environmental Protection Agency, Office of Water (EPA 815-R-99-001).

US EPA (1999b) Health effects from exposure to high levels of sulfate in drinking water workshop. Washington, DC, US Environmental Protection Agency, Office of Water (EPA 815-R-99-002).